

Soft Optomechanical Systems for Sensing, Modulation, and Actuation

Ferran Pujol-Vila, Pau Güell-Grau, Josep Nogués, Mar Alvarez,* and Borja Sepúlveda*

Soft optomechanical systems have the ability to reversibly respond to optical and mechanical external stimuli by changing their own properties (e.g., shape, size, viscosity, stiffness, color or transmittance). These systems typically combine the optical properties of plasmonic, dielectric or carbon-based nanomaterials with the high elasticity and deformability of soft polymers, thus opening the path for the development of new mechanically tunable optical systems, sensors, and actuators for a wide range of applications. This review focuses on the recent progresses in soft optomechanical systems, which are here classified according to their applications and mechanisms of optomechanical response. The first part summarizes the soft optomechanical systems for mechanical sensing and optical modulation based on the variation of their optical response under external mechanical stimuli, thereby inducing mechanochromic or intensity modulation effects. The second part describes the soft optomechanical systems for the development of light induced mechanical actuators based on different actuation mechanisms, such as photothermal effects and phase transitions, among others. The final section provides a critical analysis of the main limitations of current soft optomechanical systems and the progress that is required for future devices.

respond to one or more external stimuli (e.g., light, temperature, strain, humidity, pH or electromagnetic fields) by changing their own properties (e.g., shape, size, viscosity, stiffness, color, among others). In this framework, soft optomechanical materials have the capacity to merge the unique optical properties of plasmonic and/or photonic structures, carbon-based nanomaterials (CNMs) or macromolecules with the high tunability and elasticity of soft polymers. Given the high transparency of many soft polymers in the visible and near-infrared (NIR) spectral ranges, together with the possibility to incorporate such optical structures with high compliance in polymers that can withstand large mechanical deformations, makes this combination of optical and mechanical features ideal for the development of functional optomechanical devices.^[1]

Soft optomechanical systems can be designed to change their optical properties under mechanical stimuli induced,

1. Introduction

During the last decade, a large interest has arisen in the so-called *smart materials*, which have the ability to reversibly

for example, by strain, temperature, pH and so on, to develop cost-effective and highly sensitive sensors and optical modulators handling large strains, keeping their properties after many deformation cycles and adapting to complex and irregular surfaces. Note that, for example, sensors detecting mechanical deformations (e.g., strain or displacements) are required in structures such as buildings, vehicles, packages or wearable devices, where it is necessary to determine the experienced mechanical stress. Conversely, mechanical sensors can be used as transducers to detect other kind of external stimuli (e.g., chemical, biochemical, optical, to mention a few) that are able to produce mechanical deformations in the material. This category includes, e.g., some biosensors and micro-electro-mechanical systems (MEMS) that have been widely developed during the last decade. Soft mechanical sensors require a compliant transducer, being the electrical and optical transduction methods the most widely developed. However, optical transduction offers several advantages, particularly, its wireless detection nature, high sensitivity, easy readout, and the capacity to provide 2D strain mapping, even with sub-micron scale spatial resolution.^[2–4]


The high optical tunability of soft optomechanical systems by external mechanical stimuli can also be exploited to build mechanical modulators to modify the color or transparency of surfaces, having great potential in the development of smart windows,^[5] rewritable optical displays, encryption, and anti-counterfeiting applications,^[6] among others.^[7]

F. Pujol-Vila, P. Güell-Grau, M. Alvarez, B. Sepúlveda
Instituto de Microelectrónica de Barcelona (IMB-CNM, CSIC)
Campus UAB, Bellaterra, 08193 Barcelona, Spain
E-mail: mar.alvarez@csic.es; borja.sepulveda@csic.es

P. Güell-Grau, J. Nogués
Catalan Institute of Nanoscience and Nanotechnology (ICN2)
CSIC and BIST
Campus UAB, Bellaterra, 08193 Barcelona, Spain

J. Nogués
ICREA
Pg. Lluís Companys 23, 08193 Barcelona, Spain

M. Alvarez
Networking Research Centre on Bioengineering, Biomaterials and
Nanomedicine (CIBER-BBN)
28029 Madrid, Spain

 The ORCID identification number(s) for the author(s) of this article can be found under <https://doi.org/10.1002/adfm.202213109>.

© 2023 The Authors. Advanced Functional Materials published by Wiley-VCH GmbH. This is an open access article under the terms of the Creative Commons Attribution License, which permits use, distribution and reproduction in any medium, provided the original work is properly cited.

DOI: 10.1002/adfm.202213109

On the other hand, light can be used in soft optomechanical systems for exerting controlled local mechanical deformations as base to create new powerful and versatile actuators. The interest to develop soft stimuli-responsive actuators has recently grown considerably due to their advantages with respect to conventional hard actuators, such as their adaptability to changing environments, resiliency to high loads, easy miniaturization and low-cost. Light-responsive actuators have the advantage of offering wireless remote control with high precision and rapid modulation. Moreover, these actuators can be tailored to incorporate extra functionalities, such as biocompatibility or self-sensing. These optomechanical actuators can be used in a wide range of applications, including wireless soft robots,^[8–10] artificial muscles,^[11,12] self-regulated optical components,^[13] externally controlled switches^[14] and energy harvesters.^[15,16]

With the aim to cover all these alternatives, here we present an extensive literature review of the most representative soft optomechanical systems and their applications for sensing, modulation, and actuation, which are summarized in **Figure 1**. We first focus on the optomechanical systems for sensing and modulation, which we have grouped according to their different detection mechanisms, and next we present the soft optomechanical actuators.

2. Soft Optomechanical Systems for Sensing and Modulation

In soft optomechanical systems, the application of an external mechanical stimulus produces a variation in the optical properties that can be used either as detector of the mechanical stimulus or as modulator to tune its own optical properties. There are two main optical properties that can be exploited for detection or modulation applications: i) the changes in the

wavelength, λ (i.e., the color) of the transmitted or reflected light generated by mechanical deformations, also denoted as mechanochromic effect, or ii) the variations in the transmitted or reflected light intensity.

Mechanochromic detection relies on the interaction of light with plasmonic and/or dielectric materials that are structured at the sub-wavelength or wavelength scale. In the case of plasmonic nanomaterials, their color is given by the interaction of light with the free electrons in the metal nanostructures, which can excite localized or propagating surface plasmon resonances. On the other hand, dielectric photonic structures, such as gratings and photonic crystals (PhCs), are wavelength-scale structures, where diffraction and interference effects are predominant in the observed color. In contrast, optical detection based on light intensity variations is typically based on structures with dimensions larger than the light wavelength, such as textured surfaces, waveguides and microlenses.^[1]

2.1. Mechanochromic Systems Based on the Near-Field Interaction Between Nanoplasmonic Structures

One of the most widely used strategies to detect mechanical strains and deformations using nanoplasmonic materials is based on the strong near-field interaction between neighboring plasmonic nanostructures, which is extremely sensitive to the inter-particle distance. The near-field interaction is generated by the electromagnetic field that light induces around the plasmonic nanostructures, which has a decay length in the range of few nanometers, which enables the efficient electromagnetic interaction between nearby particles. The phenomenology can be understood as near-field interacting resonant dipoles. However, due to the finite size of the nanoparticles (NPs) and their very small separation distance, the dipole–dipole model does

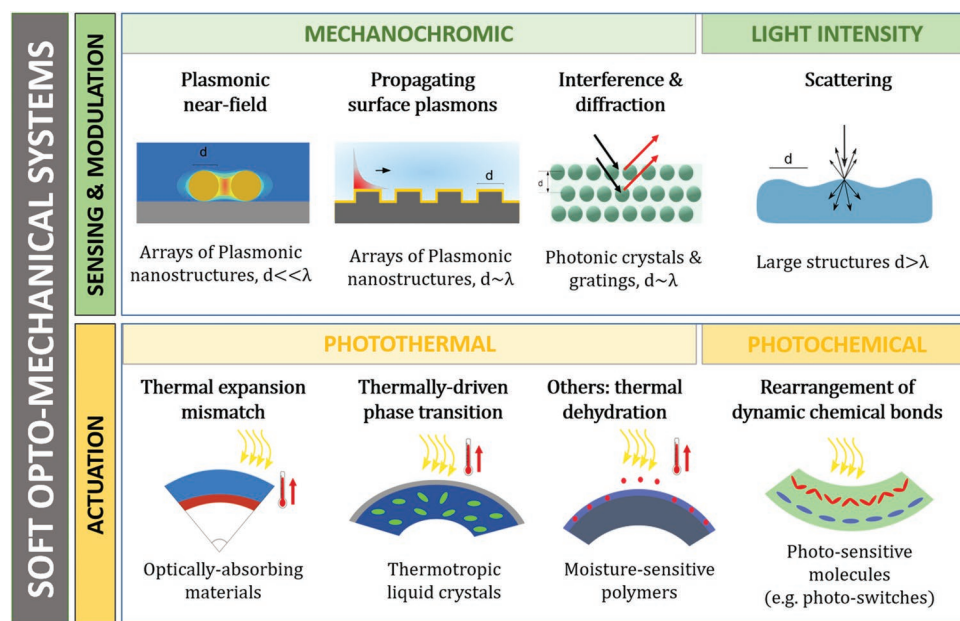


Figure 1. Schematic of the soft optomechanical systems for mechanical sensing, optical modulation and mechanical actuation, according to their different working principles.

not provide correct quantitative spectral changes, thus requiring numerical simulations, such as finite-difference time-domain (FDTD), to accurately model the electromagnetic response. In

the simplest case of two identical nearly touching plasmonic NPs, the near-field interaction (Figure 2a left panel) produces a blue-shift in their localized surface plasmon resonance when

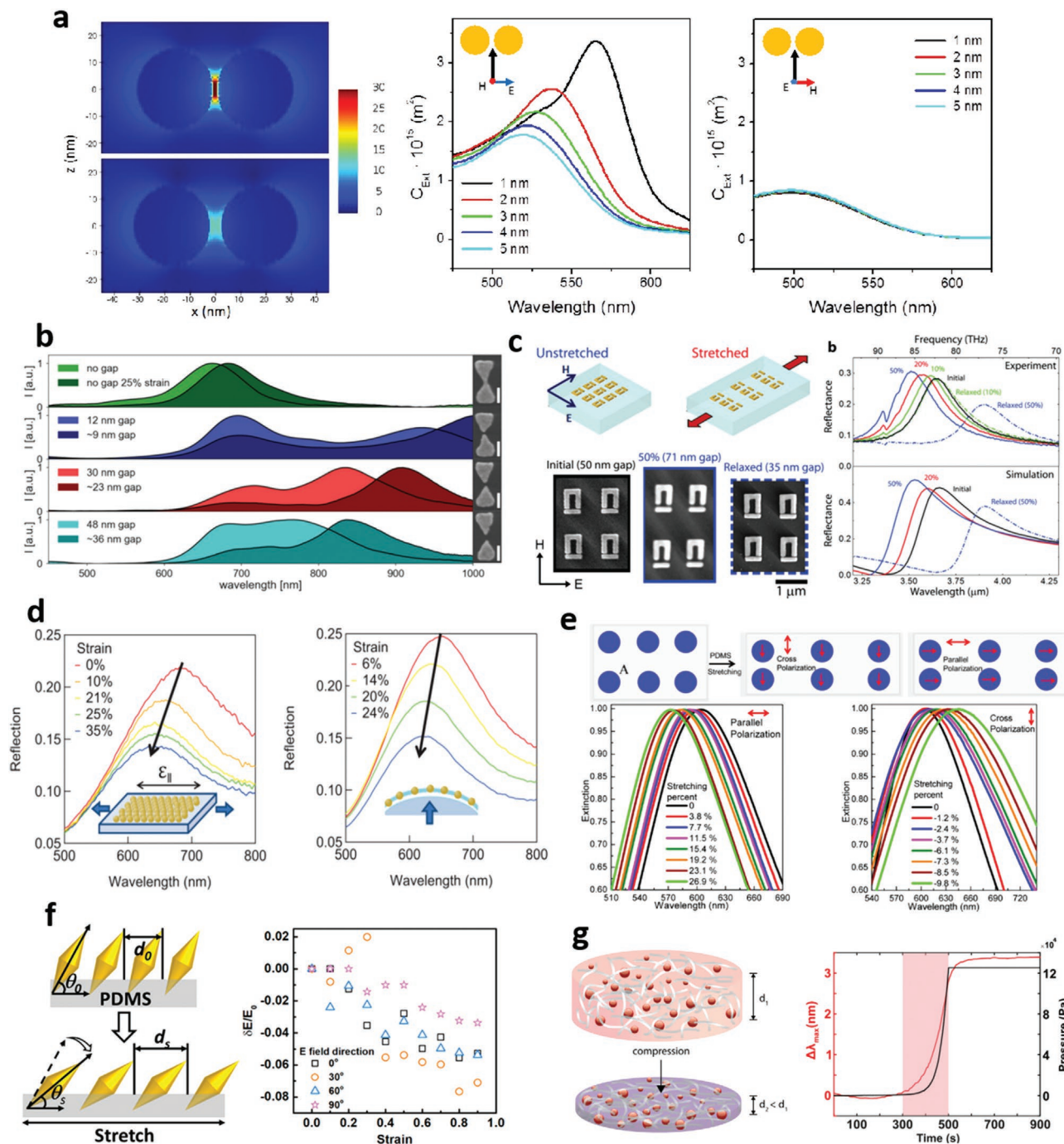


Figure 2. Strain sensors and modulators based on plasmonic near-field interaction. a) FDTD simulations of the near-field interaction between two identical nearly touching plasmonic NPs (left panel), and light extinction cross section (C_{ext}) as a function of the inter-particle distance when the light polarization is parallel (middle panel) and perpendicular (right panel) to the axis of the particle dimer. b) Optomechanical response of bow-tie antennas of different separations to 25% strain. Reproduced with permission.^[19] Copyright 2018, Royal Society of Chemistry. c) Strain-responsive split-ring resonators on PDMS. Reproduced with permission.^[22] Copyright 2010, American Chemical Society. d) Optomechanical response of 2D arrays of Au nanoparticle on PDMS to unidirectional and bidirectional strain. Reproduced with permission.^[27] Copyright 2012, AIP publishing. e) Polarization-dependent response of Ag nanodisks on PDMS. Reproduced with permission.^[28] Copyright 2015, American Chemical Society. f) Self-assembled arrays of Au nanobipyramids combining near-field and particle orientation changes under strains, reproduced with permission.^[32] Copyright 2021, American Chemical Society. g) 3D near-field interaction in arrays of plasmonic AuNPs self-assembled in nanocellulose matrices. Reproduced with permission.^[41] Copyright 2010, Wiley-VCH GmbH.

the interparticle distance increases and the light polarization is parallel to the axis of the particle dimer (Figure 2a middle panel), and red-shift when the polarization is perpendicular to the axis, being later effect much weaker (Figure 2a right panel). Therefore, quantification of the polarization dependent spectral shifts of the plasmonic resonances provides an extremely sensitive method (i.e., plasmonic ruler) to determine the changes in the separation distance between the nanostructures, as the ones produced by the stretching of an elastomeric substrate. This strategy was initially exploited by F. Huang et al.,^[17] in the case of isolated dimers of spherical gold nanoparticles (AuNPs) deposited on a stretchable polydimethylsiloxane (PDMS) substrate. In this case, the color change of the particle dimer generated by the PDMS film stretching could be detected by dark-field spectroscopy. A similar tendency in the optical resonance was shown for Au nanodiscs dimers under stretching,^[18] with a peak-shift sensitivity of 3.4 nm/% of linear deformation for tensile strain, and of 16 nm/% for compressive strain. With the aim to enhance the near field interaction between the plasmonic nanostructures and the optomechanical response under elongations, bow-tie antennas and nanorods (NRs) fabricated by stencil lithography directly on the elastomer substrates or by e-beam lithography and transferred to PDMS^[19,20] were developed (Figure 2b).

Large optomechanical effects were also shown by Pryce and coworkers for a much more complex nanoplasmonic system composed of arrays of non-interacting dimers formed by asymmetric U-shaped Au nanostructures in elastomer substrates.^[21] In these particular structures, film stretching produced both changes in the interparticle distance and geometrical deformations in the nanostructures. The combination of both effects yielded up to 400 nm red-shift (i.e., even larger than the plasmonic resonance linewidth) when the light polarization was perpendicular to the dimer, and enabled tuning the Fano-resonance of the structures. Moreover, they also analyzed the optomechanical response of split-ring resonators of different geometries under stretching, yielding wavelength tunabilities up to 400 nm (Figure 2c).^[21,22] The shape changes caused by polymer stretching were also the basis of the optomechanical response in metallic electromagnetic meta-atoms, which were fabricated using MEMS-based stencil lithography, showing mechanically tunable optical resonances in the mid-infrared.^[23]

The optomechanical changes observed in particle dimers could be enhanced in the case of particle chains. Linear chains embedded in polymer films were applied as stress-responsive colorimetric films that could memorize the experienced stress.^[24,25] The film compression induced an increase in the lateral dimensions of the film, which enlarged the interparticle distance in the chains and produced intense blue-shifts of their plasmonic resonances (working range up to 160 MPa). Exploiting this effect, a pressure sensor was developed, in which the color change of the composite material could be easily analyzed using a conventional smartphone camera.^[26]

The optomechanical response is somewhat more complex in the case of 2D arrays of plasmonic nanostructures that experience simultaneous near-field interaction in the two dimensions. This was the case of self-assembled AuNPs in a hexagonal close-packed structure deposited on an elastomer film (Figure 2d).^[27] The uniaxial film stretching induced the separation of the

NPs in the elongation direction and contraction in the perpendicular direction as a consequence of the Poisson ratio of the elastic material. These effects generated spectral shifts in opposite directions and reduced the overall observed blue-shift in the plasmonic resonance (sensitivity of 1.15 nm/%). In contrast, biaxial stretching was able to separate the distance in the two dimensions, thereby maximizing the observed blue-shifts (1.8 nm/%). Similar mechanochromic effects were observed in the case of monolayers of self-assembled silver (Ag) nanodiscs using Langmuir–Blodgett (LB) technique and deposited on PDMS substrates (Figure 2e).^[28] The plasmo-mechanical color modulation was also demonstrated in dense arrays of Ag nanocubes by biaxial stretching, which enabled active tuning the light transmitted color of unpolarized light from magenta to orange to yellow by stretching the substrate up to 20%.^[29] In a different fabrication approach, a drying-mediated self-assembly method could generate highly ordered close-packed arrays of plasmonic particles.^[30] Based on this method, periodic arrays of Au nanocubes in PDMS were fabricated, and the influence on strain sensitivity exerted by different types of polymeric ligands, interparticle distance, and size, was studied revealing a dramatic effect of these factors.^[31] Fu. et al. reported PDMS-supported self-assembled close-packed arrays of Au nanobipyramids with different orientation angles (Figure 2f).^[32] Under strain, the material exhibited simultaneous changes in particle orientations and interparticle distance displaying highly sensitive optomechanical responses, which depended on the initial orientation of the plasmonic elements (maximum strain sensitivity in $\approx 45^\circ$ oriented samples). Cataldi and co-workers studied Au nanoparticle-coated PDMS plasmomechanical sensors^[33–36] fabricated by chemical growth on the substrate, which allowed accurate control of the inter-particle gap with the number of growth cycles. Exploiting this effect, they analyzed how this material could mechanically tune the photogenerated heat by the AuNPs upon laser excitation.^[37] In the case of small 2D arrays, such as Au nanodiscs heptamers embedded on a PDMS membrane,^[38] dynamic tuning and symmetry lowering of the Fano resonances under uniaxial stress was shown by Cui et al.

The optomechanical changes could be amplified by fabricating dense arrays of plasmonic nanodisks on low-modulus, high-elongation elastomeric substrates under extreme deformations.^[39] These structures showed tunable optical response, with reversible shifts over nearly 600 nm, due to the generation of nonlinear buckling processes, which transformed the initially planar arrays into 3D configurations with rotated nanodiscs out of the plane and forming linear arrays with a wavy geometry.

The previously described soft optomechanical systems were based on the near-field interaction in one or two dimensions. However, mechanically responsive soft plasmonic materials can also be fabricated with interactions in three dimensions. For example, densely packed AuNPs embedded in a spherical silica crust and embedded in polymer film could act as mechanochromic strain sensors.^[40] When the films were stretched, the microcapsules were deformed into elongated ellipsoidal shapes and the distance between the AuNPs embedded in their shells increased, thus generating the expected resonant blue-shifts. Another 3D alternative was achieved by bacterial

nanocellulose matrices in which different types of plasmonic NPs were self-assembled. These 3D matrixes exhibited large spectral variations in response to compression,^[41] going from the typical absorption bands of the isolated NPs to nearly perfect light absorption in a broadband range, which resulted in a color change from red to almost black (Figure 2g). These nanocomposites also exhibited improved refractometric biosensing resolution, as well as amplified 2-photon absorption and photothermal effects in the compressed samples. On the other hand, decorating AuNPs on poly(*N*-isopropylacrylamide) (PNIPAM) microgels exhibited reversible color shifts (between red and grayish violet) in response to a temperature changes,^[42] due to the mechanical deformation of the polymer particles (due to thermal expansion) and the induced resonance red-shifts. This optomechanical concept was applied as thermometers with a temperature resolution of 0.2 °C, and freestanding colorimetric patches were utilized as spatial temperature scanners, which could potentially be applied to wearable sensors. Following this trend, pH-sensitive hydrogels containing embedded AuNPs were demonstrated,^[43] as well hydrogel nanofiber waveguides containing Au NRs for humidity sensing.^[44]

2.2. Mechanochromic Systems Based on Propagating Surface Plasmons

In contrast to near-field interacting small plasmonic NPs, periodic arrays of plasmonic nanostructures whose size is in the same range of the light wavelength can excite propagating plasmon modes, and their excitation condition can be tuned when the arrays are mechanically deformed.

This approach was used in the case of Au-coated nanovoids (diameter 900 nm) in PDMS, in which the plasmonic periodic nanostructures supported localized and propagating plasmon modes.^[45] This system exhibited a broad resonance and it could be stretched up to 5% strain, yielding resonance redshifts with a sensitivity of 3 nm/%.

In addition, arrays of hexagonal close-packed polystyrene nanospheres capped by Ag and Au layers on PDMS were reported by Zhu X et al.^[46,47] (Figure 3a). In this case, the proximity between particles and their periodicity enabled the generation of delocalized propagating plasmonic modes that were strain- and angle sensitive. When the material was stretched, two properties changed simultaneously: the distance and near-field interaction between the metallic caps and lattice pitch in the elongation directions, which produced a redshift and broadening of the plasmon resonance (sensitivity 1.33 nm/%).

Strain-sensitive Au nanolines on flexible substrates constituted an example of plasmonic periodic structures in one dimension (Figure 3b).^[48] Instead of conventional lithographic techniques, in this work, AuNPs were self-assembled in ridges and annealed to form the nanolines. As in the previous cases, the films stretching produced a redshift of the plasmonic resonance. In another example, periodic arrays of asymmetric “U-shaped” aluminum-coated polyurethane nanowires showing Fano resonances were investigated by Lütolf et al. (Figure 3c).^[49] In these structures, the electromagnetic field could be guided in the direction perpendicular to the nanowires and their reso-

nance experienced a redshift and a steep decrease on the amplitude upon increasing strain. The scalability of the fabrication enabled the fabrication of large arrays in which the strain was translated into macroscopic colorimetric changes that could be easily analyzed, e.g., for 2D strain mapping.

Another interesting example involving propagating surface plasmons was reported by Yoo et al.^[50] by using tunable plasmonic arrays of Au-coated asymmetric PDMS micropylramids, in which film stretching yielded a change in the angle between the pyramid facet and the incident light (Figure 3d). Due to the high angular sensitivity in the excitation of the propagating surface plasmon via total internal reflection on the pyramidal facets, this material could achieve an outstanding sensitivity of 15.22 nm for a 1% strain (i.e., 15.22 nm/% sensitivity), thus showing the largest strain spectral response reported to date.

Interestingly, mechanical engineering can be used to amplify the strain in specific regions and, therefore to enhance the optomechanical response of plasmonic metamaterials.^[51] This effect was achieved by a reconfigurable metasurface constructed by a plasmonic lattice array in the gap between a pair of symmetric microrods that served to locally amplify the strain created on the elastomeric substrate by an external mechanical stimulus. The strain on the metasurface could be amplified up to 15.9-fold with respect to the external strain by tailoring the microrod geometry, thereby enhancing the mechano-sensitivity of the optical responses.

2.3. Mechanochromic Systems Based on Other Nanoplasmonic Interactions

In addition to the near-field interaction between localized plasmonic resonances, the optical anisotropies in elongated plasmonic nanostructures can be also combined with elastic matrices to generate enhanced optomechanical functionalities.

Xu et al.^[52] reported a Au NRs/hydrogel composite that displayed a polarization-dependent light absorption upon stretching due to the alignment of the plasmonic elements (randomly dispersed in the unstretched composite) (Figure 4a). Additionally, the non-aligned configuration could be recovered by photolithographic patterning, with potential applications in polarized displays and encryption.

On the other hand, the catalytic activity of Au nanostructures was used to generate the first wrinkled plasmonic enhanced Fabry-Perot (FP) elastic cavities.^[53] The cavities were spontaneously formed by thermally curing the PDMS on arrays of plasmonic nanodomes, thereby inducing their penetration at controlled depths inside the polymer matrix and generating a stiffness gradient. The combination of both effects yielded tunable corrugated FP cavities, which simultaneously exhibited large wavelength and intensity variations in the FP optical resonances (Figure 4b). The analysis of both parameters enabled achieving a high sensitivity (2.21 nm/%) and an unprecedented strain detection limit of 0.006%. Mechanically tunable FP cavities could also be obtained by elastomeric dielectric films sandwiched between two metal layers, which could have potential for structural health monitoring.^[54]

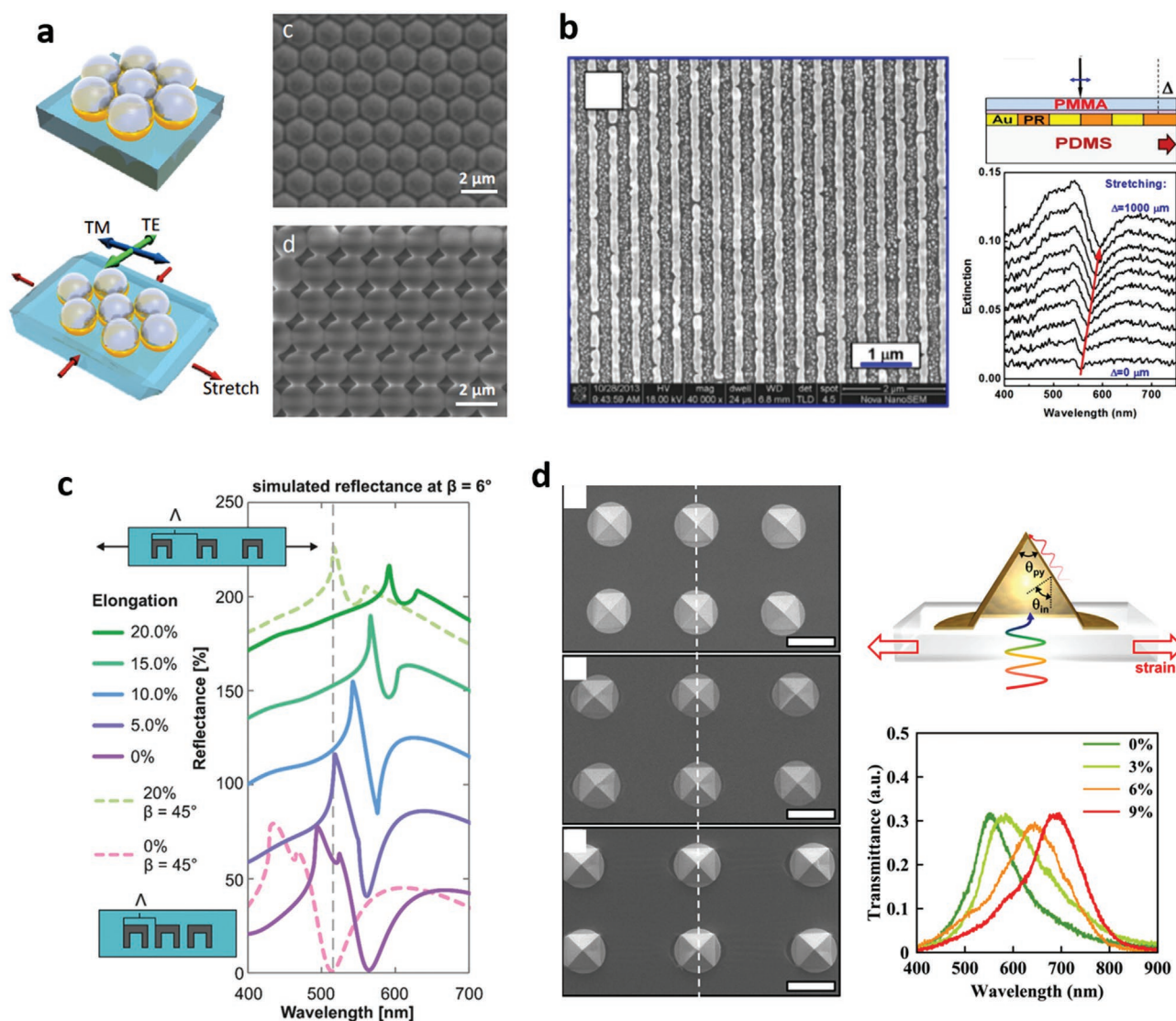


Figure 3. Strain sensors and modulators based on surface propagating plasmons. A) Array of Au-capped polystyrene nanospheres on PDMS. Adapted from.^[47] b) Optomechanical response of Au nanolines on PDMS. Reproduced with permission.^[48] Copyright 2014, Springer Nature. c) Optomechanical response of U-shaped, aluminium-coated polyurethane nanowires. Reproduced with permission.^[49] Copyright 2016, Wiley-VCH GmbH. d) Array of Au-coated micropyramids in PDMS and corresponding optomechanical response. Scale bar 20 μm. Reproduced with permission.^[50] Copyright 2015, American Chemical Society.

2.4. Mechanochromic Systems Based on Light Interference and Diffraction

Light diffraction and interference generated by a periodic contrast of refractive index at the wavelength scale, as in diffraction gratings and photonics crystals, produce a structural coloration in the material. Mechanical deformation in the ordered structure generates a mechanochromic effect, which can be used for developing sensors to detect mechanical deformations caused by strain or other stimuli capable to change their periodicity (e.g., swelling).

In the case of diffraction gratings, the diffracted light by the periodic grooves at the surface of the material causes a wavelength separation of the transmitted and reflected light in different angles, which is very sensitive to variations in the

periodicity and the angle of incidence, following the diffraction equation:^[55]

$$m\lambda = d(\sin \alpha + \sin \beta) \quad (1)$$

where α is the incident angle, β is the reflection angle, d is the periodicity, m is the diffraction order ($m = 0, \pm 1, \pm 2, \pm 3, \dots$), and λ is the wavelength. Nanoimprint lithography (NIL) offers an easy, low-cost methodology to produce large area diffraction gratings,^[56,57] and its use for mechanochromic sensing have been reported by several authors. For example, colorimetric pressure sensors were proposed,^[58–60] which could be applied in non-contact intraocular pressure sensing.^[59] Diffraction gratings have also been exploited as self-sensing mechanism to quantify the mechanical actuation in soft-robotic structures,

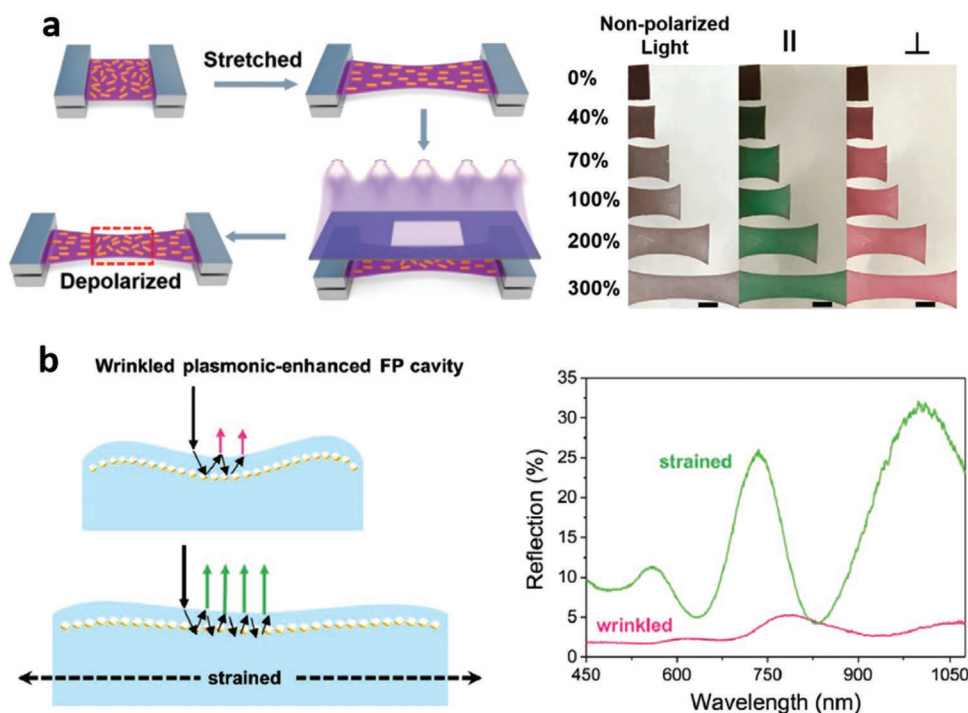


Figure 4. Strain sensors and modulators based on other plasmonic interactions. a) Polarized display composed of Au NRs embedded on elastomeric films that align the NRs under film stretching. Reproduced with permission.^[52] Copyright 2020, Wiley-VCH GmbH. b) Elastic plasmonic enhanced wrinkled FP cavities obtained by self-embedded Au nanodomains in PDMS films, showing intense blue-shifts and intensity increase in the cavity resonances under film stretching. Reproduced with permission.^[53] Copyright 2022, Wiley-VCH GmbH.

driven by pneumatic pressure^[61] or temperature (by using shape memory alloy wires).^[62] Diffraction-based coloration was also exploited to wirelessly detect the deflections of cantilever-shaped soft optomagnetic actuators.^[63] This opto-magneto-mechanical system was composed of a nanostructured-iron (Fe) film mechanically linked to a periodically corrugated thin PDMS film, thereby enabling synergistic optical and magnetic actuation and simultaneous colorimetric detection (Figure 5a), with a detection limit of 1.8 mW cm^{-2} and 0.34 mT respectively, by a simple color imaging analysis in a conventional smartphone camera. A similar colorimetric detection method was used in PDMS cantilevers with one grating surface to monitor reversible molecular conformational changes of an azobenzene monolayer when exposed to Ultraviolet (UV) light, showing similar sensitivity to the traditional beam detection method ($4.6 \times 10^{-3} \text{ N m}^{-1}$).^[64] Following this trend, versatile strain sensors based on elastomeric 2D arrays of cone-shaped structures enabled measuring biaxial and shear strains with high performance.^[65] Another alternative to develop diffraction gratings is the use of 2D arrays of self-assembled polystyrene microspheres as a template. This strategy was followed to fabricate periodic 2D structured elastomeric membranes as colorimetric pressure sensor for optofluidic applications.^[66] A sensitivity of 0.17 kPa^{-1} was obtained by measuring the diffracted color changes induced by the membrane deformation.

Alternatively, the linear buckling theory^[67] has also been exploited to fabricate periodic textured surfaces on elastic polymers, based on the mechanical strain between two contacting materials of different Young's modulus, which spontaneously produce surface buckles to minimize the surface energy arising

from their differential deformation. The generation of periodic surface wrinkles on PDMS by an oxygen plasma treatment in an initially stretched PDMS was proposed for the design of mechanochromic devices featuring bright structural colors and programmable colorimetric responses.^[68–70] Further advancing in this concept, Xu et al. demonstrated the fabrication of micro-prism arrays and diffraction gratings of different geometries using shape memory polymers and its posterior optomechanical analysis to build shape-memorizing micro-optics^[71] (Figure 5b).

Diffraction induced colored materials were also produced by using soft 2D arrays of plasmonic nanostructures, where far-field interference among individual nanostructures of the lattice suppressed all the scattered light outside the specified wavelength window.^[72] Using this mechanism, vivid colors that can be tuned across the entire visible spectrum were produced by stretching in its two dimensions an array of Al plasmonic nanodiscs on top of a soft substrate. Similarly, a square array of Au capped PDMS nanopillars on an elastomer substrate was used to study the inverse optical behavior between polarized light parallel and perpendicular to the stretch axis.^[73]

In contrast to diffraction gratings, PhCs in 1D, 2D, and 3D can prevent the propagation of light at certain wavelengths (photonic bandgaps), presenting an intrinsic structural color defined by Bragg's and Snell's law:^[74]

$$\lambda_{\max} = \frac{2}{m} d \sqrt{n_{\text{eff}}^2 - \sin^2 \alpha} \quad (2)$$

where λ_{\max} is the wavelength at which maximum reflection occurs, α is the incident angle, m is the diffraction order

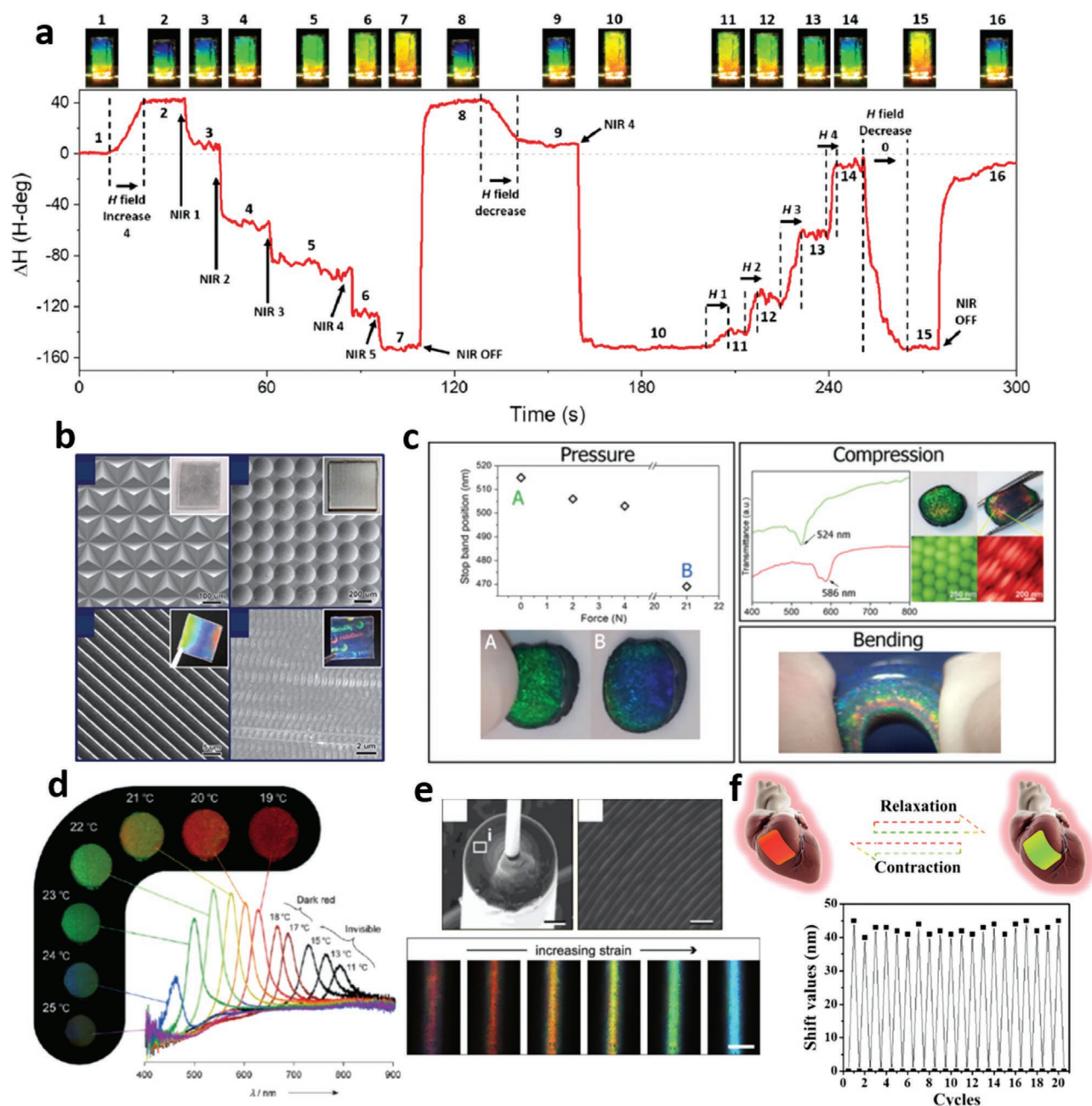


Figure 5. Optomechanical mechanochromic systems based on diffraction gratings and PhCs. a) Colorimetric detection of opto-magnetic and periodically corrugated cantilevers enabling optical and magnetic actuation. Reproduced with permission.^[63] Copyright 2021, American Chemical Society. b) SEM image of different micropatterned shape-memory polymers for programmable micro-optics. Reproduced with permission.^[71] Copyright 2013, Wiley-VCH GmbH. c) Graphene-infused block co-polymer PhCs. Reproduced with permission.^[94] Copyright 2020, Wiley-VCH GmbH. d) Thermally-adjustable photochromic hydrogel spectrometry and representative images. Reproduced with permission.^[96] Copyright 2007, Wiley-VCH GmbH. e) Mechanochromic elastic fiber based on a bio-inspired multilayer of PDMS/PSPI. Reproduced with permission.^[115] Copyright 2013, Wiley-VCH GmbH. f) Bioinspired structural color patch. Reproduced with permission.^[121] Copyright 2020, American Association for the Advancement of Science.

($m = 0, \pm 1, \pm 2, \pm 3, \dots$), d is the lattice constant, and n_{eff} is the effective refractive index of the crystal.

This effect enables generating selective macroscopic colors by regulating the center wavelength of the bandgap, thereby being very sensitive to changes in the refractive index and periodicity.^[75] Soft 1D PhCs, consisting of alternating high and low refractive index materials, have demonstrated mechanochromic

effect with a sensitivity over 6 nm/% strain.^[76] By embedding a 1D PhC formed by periodically arranged dielectric NRs in a deformable PDMS substrate, different planar strains could be identified, including their application direction, type, and value.^[77]

2D PhCs composed of periodic cylinder-shaped air holes in a triangular lattice, made in PDMS by NIL could distinguish

four strain ranges below 50% of strain, from 0% to 6.7% (red), 6.7%–13% (yellow), 13%–30% (green), and 30%–50% (blue).^[78] On the other hand, 2D PhCs based on 2D arrays of self-assembled particles were also applied to develop strain-sensors and other mechanochromic devices. For example, color writing in photonic “papers” with totally transparent materials was proposed by Fudouzi et al.,^[79] which were based on 2D PhCs whose interparticle distance and coloration varied due to the swelling induced by the local application of an organic solvent.

The majority of the strain sensitive soft 3D PhCs, also referred as opals, are based on the 3D self-assembly of polystyrene or silica nanospheres,^[80] followed by the infiltration of the elastic polymer matrix (such as PDMS) and a posterior etching of the spheres. The works of Weismann et al.^[81] and Fudouzi et al.^[82,83] demonstrated the strong colorimetric response of the opal structures to the applied mechanical strain. In the case of close-packed arrays of latex particles embedded in PDMS, the reflected color blue-shifted to shorter wavelengths (the peak position moved from 589 to 563 nm) due to the decreased distance between particles in the direction perpendicular to the uniaxial stretching (up to 20% elongation).^[83] This strategy was followed by several authors that studied in detail the diffraction phenomena in distorted crystal lattices,^[84] and optimized the fabrication process to achieve more robust and reversible actuation.^[85] The use of different soft materials, such as hydrogels,^[86] photocurable and shape-memory polymers,^[87–89] or block copolymers^[90] have also been investigated. For example, multilayered films of silica particles in elastomeric polyacrylates displayed a remarkable linear blue-shift in the reflected color from 568 to 496 nm under uniaxial strain of 50%, caused again by the reduction in the inter-particle distance in the direction normal to the strain.^[89] Yang et al. used metastable 3D SiO₂ colloidal crystal array, fixed in a mixture of ethylene glycol and poly(ethylene glycol)-methacrylate through photopolymerization, to develop a colorimetric force sensor with high sensitivity ($\Delta\lambda = 150$ nm for 12% stretch and 22% shrink) and fast response (20–200 ms), which was also applied as efficient mechanically-modulated color display screen.^[91] In an interesting approach, Lee et al.^[92] prepared elastic photonic microbeads based on silica particles and a photocurable polymer, which were used as building blocks to obtain mechanochromic materials displaying angle-independent color changes as individual microbeads dynamically deform under macroscopic strain. In addition, hybrid systems combining PhCs and 2D materials such as graphene have been explored.^[93] For instance, graphene-infused block co-polymer PhCs displayed a remarkable thermochromic and mechanochromic performance,^[94] as shown in Figure 5c. The mechanochromic response of the opal structures was also exploited to develop other applications. For example, an elastomeric opal was used to tune the photoluminescent emission of PbS quantum dots by the application of pressure.^[95] Hydrogel opals have been of great interest to develop thermoresponsive colorimetric sensors, based on the high thermal expansion of hydrogels that causes the isotropic deformation of the crystal lattice, thereby producing large color shifts^[96] (Figure 5d). Following a similar strategy, other types of sensors have been developed, such as biosensors^[97] or magnetic field detectors,^[98,99] among others.^[100] In general terms, these sensing approaches take advantage of the fast hydrogel

swelling/shrinking induced by chemical interactions.^[86] For example, using pH-sensitive hydrogels, high-performance pH determinations were achieved,^[101] as well as multi-responsive photonic nanochains for microenvironment analysis.^[102] Going further, chemical modifications of photonic hydrogels enabled selective detection of specific molecules such as glucose,^[103–105] and proteins,^[106] among others.

On the other hand, hydrogel sensors based on thin-film interference have also been showcased, in which the fast hydrogel swelling is translated into changes in the film thickness and thus into a shift in its reflected color.^[107] In thin-film interference, the constructive interference becomes $m\lambda = 2n_2d\cos\theta_2$ for $n_1 < n_2$, where λ is the wavelength giving the maximum reflectivity, d is the film thickness, n_2 is the refractive index, θ_2 is the angle of refraction, and m is an integer. In a remarkable work, Qin et al. reported on a hydrogel interferometer as a facile approach for colorimetric humidity assessment, volatile-vapor sensing, and breath-controlled information encryption.^[108]

Biomimetic micro and nanostructures inspired by some living organisms have been used to develop soft optomechanical sensors and color modulators. For example, *Morpho* butterfly wings are composed of a complex tridimensional microstructure that presents iridescence. Various authors explored the replication of these structures to build 2D and 3D soft photonic nanostructures,^[109–111] and even combine them with metal coatings,^[109] plasmonic NPs^[112] or carbon nanotubes (CNTs)^[111] to achieve IR-responsiveness, reaching temperature detection limits of 18 mK. The multilayer structure in tropical fish scales was mimicked by multilayers of hydrolyzed polyacrylamide hydrogel and highly reflective polymerized poly(dodecyl glyceryl itaconate) platelets to achieve ultrafast color switching time (switching rate ≈ 0.1 ms), full-color tunable range, and high spatial resolution (80 μm).^[113,114] Moreover, the concentric PhCs that mimics the hierarchical photonic structure found in the seed coat of *Margaritaria nobilis* fruits was fabricated by a rolling technique with PDMS and a triblock copolymer (PSPI). This soft photonic structure was used as a band-gap tunable mechanochromic optical fiber^[115] (Figure 5e). More recently, the complex photonic structures found in color-changing animals such as chameleons and cephalopods have inspired the design of high-performance mechanochromic systems,^[116] by generating high-refractive index contrast PhCs,^[117] stiffness gradients,^[118] and combining structural color and molecular light absorption.^[119,120] Remarkably, Wu et al. reported a mechanochromic and thermochromic material mimicking the chameleon skin based on periodic arrays of colloidal particles with high-refractive index contrast, which blue-shifted more than 200 nm by a 20% compression or a temperature increase from 30 to 55 °C.^[117] As a step forward, Wang et al. developed a bioinspired structural color patch for biomedical applications based on a hydrogel inverse opal with anisotropic surface adhesion and self-reporting capability^[121] (Figure 5f). Interestingly, hybrid photonic hydrogels were suitable for monitoring the beating activity of embedded cardiomyocytes,^[93,122] and even to design self-reporting cardiomyocyte-driven soft robots.^[123]

In recent years, cholesteric liquid crystal (ChLC) elastomers have emerged as radically different materials to build soft mechanochromic devices. The ChLC phase presents intrinsic

periodicity due to its helical supramolecular structure with a pitch that can be in the range of a few hundred nanometers, thus leading to a circularly polarized structural color.^[124] Such supramolecular organization can be obtained by doping the nematic matrix with chiral molecules.^[125–127] So far, such systems have demonstrated a high performance in strain-responsive devices,^[128–130] reversible multi-responsive color displays,^[131–133] edible colored hydrogels,^[134] and elastomeric fibres for mechanochromic textiles.^[135]

2.5. Optomechanical Systems Based on Light Scattering Modulation

When light interacts with textured surfaces whose texturing dimensions are comparable or larger than the light wavelength, the induced scattering leads to a decrease in the transmitted and reflected light in the normal direction. The mechanical deformation of the textured surfaces can change the scattering pattern and, consequently, the intensity of the transmitted or reflected light, thereby being appealing to develop soft optomechanical sensors and modulators. To fabricate textured surfaces on elastic polymers, the buckling effects explained in the previous section can be used.

Several authors used the wrinkle generation strategy in PDMS to build devices with mechanically-modulated transparency,^[7] which have potential to develop smart windows,^[5,136]

rewritable optical displays, or anticounterfeiting applications,^[6] among others. For example, Kim et al. fabricated unidirectional and bidirectional wrinkling patterns and demonstrated the capacity to dynamically tune the optical diffraction and their use as switchable screens and windows^[137] (Figure 6a). The same principle was exploited by Shrestha et al., by fabricating a wrinkled pattern of a ZnO thin film on PDMS to build a mechanically tunable window.^[138] In addition, a dynamic micromirror with mechanically tunable reflection was developed by using an aluminum thin film coating as stiff layer on a shape memory polymer.^[139,140] Li et al. demonstrated a very wide range of transparency tuning by combining the surface wrinkles and the microcracks that occur on the surface due to high strains (Figure 6b).^[141] In this context, a surface wrinkled poly(vinyl alcohol) (PVA)/PDMS bilayer was also demonstrated as a mechanically switchable transparency material^[142] (Figure 6c). Taking advantage of the hydrophilicity of PVA, a mechanical stress could be generated by an increase of ambient humidity. A similar phenomenon was demonstrated by the thermal expansion of the material. Furthermore, Zeng et al. described the fabrication of three wrinkled PVA/PDMS bilayers with different response and dynamics to ambient moisture, which could be applied as water indicators or anticounterfeit tabs.^[143]

On the other hand, more complex nanostructures have been fabricated in combination with microscale surface wrinkles. For example, Lee et al. described the fabrication of a wrinkled

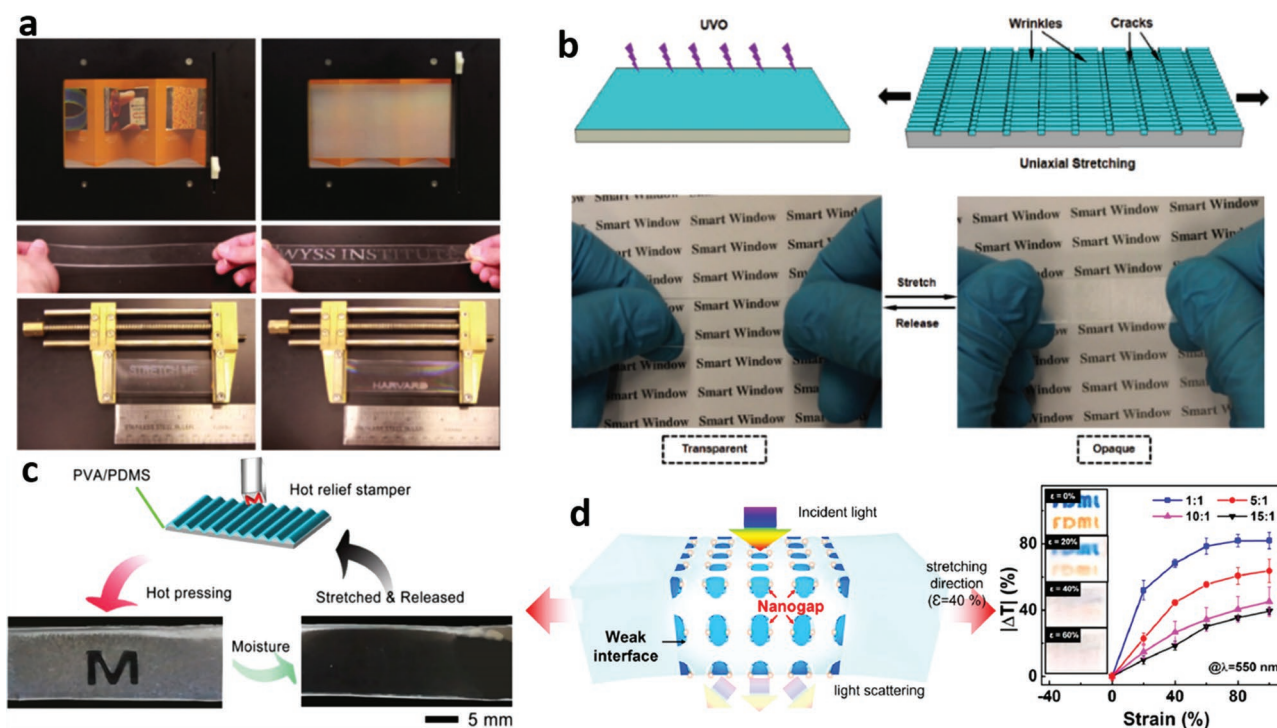


Figure 6. Optomechanical systems based on light scattering modulation. a) Mechanically-tunable switched transparency of wrinkled PDMS and proof of concept as dynamic window and switchable display. Reproduced with permission.^[137] Copyright 2013, Wiley-VCH GmbH. b) Switchable transparency in PDMS based on the formation of surface wrinkles and microcracks. Reproduced with permission.^[141] Copyright 2017, Wiley-VCH GmbH. c) Image of surface wrinkled PVA/PDMS film to develop switchable displays. Reproduced with permission.^[142] Copyright 2019, American Chemical Society. d) Schematic of the nanogap heterogeneous nanocomposite and the light transmission changes induced by the film stretching. Reproduced with permission.^[149] Copyright 2022, American Chemical Society.

PDMS film containing an array of nanoposts.^[144] They used a template of nanoporous anodic aluminum oxide to fabricate the nanoposts by replica molding, followed by PDMS stretching and UV-ozone surface treatment. They demonstrated a high sensitivity of the transparency to mechanical strain, as well as reversible hydrophobicity (and thus self-cleaning capabilities) due to the nanopost patterning. On the other hand, hierarchical surface wrinkles were proposed to achieve smaller wrinkle patterning and therefore structural coloration, in addition to tunable transparency.^[68,145] In this line, some works have exploited the combination of surface wrinkles and cracks with structural color^[146,147] or fluorescent dyes^[148] to generate mechanically switchable color digit displays. Based on these effects, Chen et al. reported periodic 3D structures composed of two interdigitated PDMS phases with different Young's modulus. Under strain, numerous nanogaps emerged between the phases acting as light scattering centers, rendering a high-contrast mechanical modulation of the light transmittance^[149] (Figure 6d).

Finally, surface wrinkled elastomeric materials have been used as template to build metal nanowires with tunable plasmonic resonances in the NIR.^[150] On the other hand, the combination of wrinkled elastomer with CNTs could generate NIR-responsive dynamic wrinkling patterns for various optically-controlled devices.^[14]

3. Soft Optomechanical Structures for Actuation

Unlike previous sensing applications in which an external mechanical stimulus induces a change in the optical properties, light stimuli can be used to generate controlled mechanical actuations in optomechanical systems. The main physicochemical principles of the optomechanical response of soft actuators are i) photothermal effects and ii) light-mediated rearrangement of dynamic chemical bonds (e.g., cis-trans isomerization).^[151,152]

3.1. Soft Optomechanical Actuators Based on Photothermal Effects

Soft actuators driven by photogenerated heat are generally composed by a soft matrix (usually polymer or gel) and a photothermal agent, which can be based on inorganic materials (e.g., plasmonic NPs), CNMs or organic dyes.^[153] In the case of metallic NPs, almost all the energy absorbed from the incident light is transformed into heat. The light absorption results from the photon energy dissipation due to inelastic processes, which warm up the whole metal lattice structure. The amount of heat (Q) generated by the light absorption can be obtained directly from the absorption cross section (C_{abs}) and the incident light irradiance (I) (i.e., light power per unit surface). CNMs have excellent light absorption over a wide range of wavelengths and excellent light-to-heat conversion efficiency. When light interacts with CNMs, the photon energy absorbed leads to the photoexcitation of electrons (if higher than the optical bandgap), whose energy is then transferred to the lattice by electron-phonon coupling, which produces heat.^[154] In organic dyes, the irradiation leads to excited states, that relax to the intermediary state, and then dissipate via radiative transi-

tion (emitting fluorescence), non-radiative decay (heat generation) or intersystem crossing. To optimize their thermal effect, improving the extinction (absorption and scattering) coefficient is usually a preferable pathway.^[155]

The conversion of the photogenerated heat into mechanical work is usually based on: i) a differential thermal expansion between the photothermal layer and the substrate, ii) a thermally-driven phase transition of the soft substrate or iii) differential changes in the humidity of the actuator.

3.1.1. Soft Actuators Based on Differential Thermal Expansion

Photothermal actuators driven by the differential thermal expansion are mainly composed of two layers of different materials (i.e., bimorph actuators) that have a large mismatch on their coefficients of thermal expansion (CTE). The differential volume expansion induced when the bilayered material is heated, produces a mechanical stress that generates the bending of the actuator. The magnitude of the mechanical actuation is directly proportional to the difference in CTE and the temperature increase.^[156] The differential expansion of each layer can be calculated by:

$$\Delta L_i = L \cdot \alpha_i \cdot \Delta T \quad (3)$$

being L the original length, α the CTE and ΔT the temperature variation. Sub-index i represents each individual layer. Therefore, the difference in the CTE (α) between both materials generates a mechanical stress, inducing the cantilever deflection in the direction of the material with lower CTE. For a bi-material system, the temperature induced bending can be estimated using its radius of curvature, r , which depends on the stress from the temperature change (ΔT) and the residual stress that may be present in the material layers. It can be calculated by:

$$r = \frac{\left[(E_1 t_1^2)^2 + (E_2 t_2^2)^2 + 2E_1 E_2 t_1 t_2 (2t_1^2 + 3t_1 t_2 + 2t_2^2) \right]}{[6E_1 E_2 t_1 t_2 (t_1 + t_2)(\alpha_1 - \alpha_2) \Delta T]} \quad (4)$$

where t_i is the thickness of each layer, and E_i is the Young's modulus of the i th layer.

In general, polymers and elastomers present very high CTE, while metals and CNMs have very low or even negative CTE.^[157] Therefore, many authors have used composite materials made of plasmonic or carbon nanostructures as photo-thermal responsive layer and a soft polymer as layer with high CTE.

As example of plasmonic based actuators, Shi et al. developed a bilayer of AuNPs mixed on poly(*N*-isopropylacrylamide) (PNIPAM) and poly(acrylamide) (PAAm).^[158] In this system, AuNPs were heated upon irradiation at the plasmon resonance wavelength, which produced the differential thermal expansion between both layers. This effect was enhanced by the desorption of water molecules from the polymer surface. Plasmonic resonances are especially interesting to achieve wavelength selectivity. In this line, an actuator based on Au NRs on PMMA was demonstrated^[12] (Figure 7a). The rational tuning of the NRs dimensions made possible building an actuator with regions that were sensitive to different wavelengths in the visible and

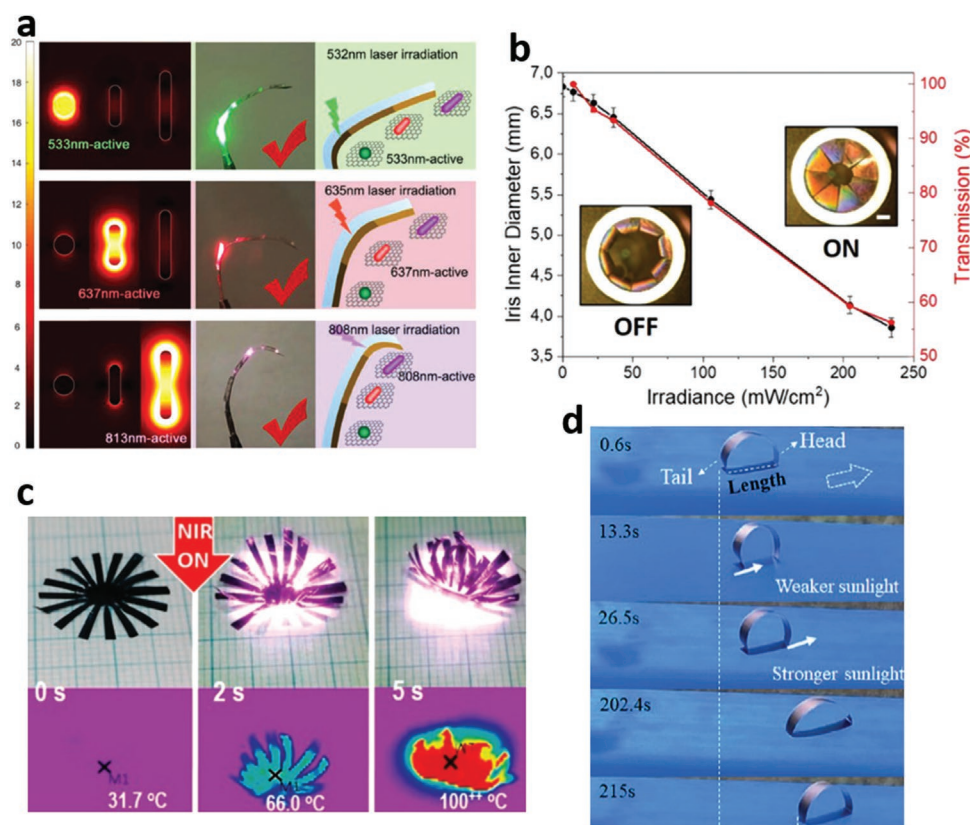


Figure 7. Soft actuators based on photothermally driven differential thermal expansion. a) Multi-wavelength responsive actuator based on gold NRs. Reproduced with permission.^[12] Copyright 2012, Wiley-VCH GmbH. b) Optomechanical response of an ultrabroadband absorption nanostructured-Fe/PDMS self-regulated iris. Reproduced with permission.^[160] Copyright 2021, Elsevier. c) Venus flower-like PEDOT-PDMS actuator under NIR irradiation. Reproduced with permission.^[175] Copyright 2017, Springer Nature. d) Self-locomotive soft actuator based on asymmetric microstructural Ti₃C₂T_x MXene film driven by natural sunlight fluctuations. Reproduced with permission.^[182] Copyright 2021, American Chemical Society.

NIR. Also, Chen et al. encapsulated copper NRs in a PVA matrix to build wavelength-dependent actuators.^[159] In contrast, highly damped plasmonic nanostructures could be designed to achieve ultrabroadband light response. This was demonstrated by mechanically-coupled arrays of Fe nanodomes transferred to thin PDMS layers to build soft actuators that could respond to light from the UV to the thermal infrared, which was applied to develop a self-regulated iris, an optical gripper and an optomechanical electrical switch (Figure 7b).^[160] In another strategy, Li et al. reported a magnetic-plasmonic actuator composed of hybrid Fe₃O₄/Ag NRs and photocurable polymer that could be modulated by switching the laser polarization.^[161] A self-locomotive bipedal soft robot driven by the light polarization was demonstrated by magnetically controlling the orientation of the NRs.

CNMs have been also widely used to build bimorph actuators. For instance, graphene oxide (GO) has been deposited on polymers like as PDMS or PMMA to develop actuators in applications such as a light-controlled electrical switch, a smart curtain that self-folds due to the sunlight irradiation, crawler and swimming robots, and NIR-responsive origami structures.^[162–165] Gao et al. took advantage of the water absorption/desorption effects to produce the opposite movement of the light induced actuation for constructing a bi-functional mechanical gripper.^[166] Furthermore, GO sheets have been combined with other photo-

thermal agents to offer extra capabilities. As examples, Yang et al. incorporated AuNPs in poly(dopamine) (PDA) to achieve an enhanced responsivity of the actuator,^[167] Zhang et al. combined nano-sized graphite and polyvinylidene fluoride (PVDF) with GO forming a dual-responsive (moisture and light) bilayer structure,^[168] and Luo et al. developed a microwave-absorbing hollow carbon spheres/GO/PDMS photothermal actuator for military applications.^[169] GO has also been combined with CNTs in PDMS to achieve dual movement and twisting due to thermally-induced actuation and water desorption.^[170] Single-wall carbon nanotubes (SWCNTs) have been also used to build photothermal actuators.^[171,172] Their optical absorption is highly dependent on the nanotube chirality, which has been exploited to develop a multi-wavelength responsive actuator.^[173] In addition, a CNTs/PDMS curled droplet-shaped actuator rendered a continuous phototactic self-locomotion, being also appealing for energy harvesting.^[174]

Other photothermal agents have been applied in this type of photothermal actuators. For example, a trilayered actuator made of carbon black ink on polyethylene terephthalate (PET) and an acrylic layer was developed.^[15] In this approximation, the combined actuation of thermal expansion and water desorption was demonstrated to build a mechanical gripper, a crawling robot and a solar-driven mill, being appealing for innovative energy harvesting approaches. Examples of

other photothermally driven actuators include the development of an artificial NIR-responsive Venus flytrap based on a poly(3,4-ethylenedioxythiophene) (PEDOT) on PDMS bilayer (Figure 7c)^[175] and a leaf-inspired, $(\text{Ti}_3\text{C}_2\text{T}_x)$ -cellulose composite on a polycarbonate (PC) membrane. In the latter example, different photothermally driven devices were built, such as a worm-like robot, a light-controlled electrical switch, or applications in displays and camouflage.^[176] Following this trend, the high photothermal efficiency of MXene materials (e.g., $\text{Ti}_3\text{C}_2\text{T}_x$) has been used of to build sharp bilayer actuators.^[177–180] For example, Luo et al. reported multifunctional $\text{Ti}_3\text{C}_2\text{T}_x$ /polyethylene soft robots accurately driven by NIR, electricity, and heat.^[181] In a different approach, a bimorph structure composed of an MXene-based asymmetric layered microstructure and polyethylene was reported, which demonstrated directional self-locomotion driven by natural sunlight (Figure 7d).^[182] Besides, a bioinspired soft actuator made from MXene-doped polydiallyldimethylammonium chloride served as artificial muscle to photothermally actuate a PhCs film and achieve a dynamic structural color imaging system.^[183] More recently, novel photothermal agents have been explored to combine various functionalities, such as magnetic self-sensing by using Fe_3O_4 ^[184] or NdFeB particles,^[185] or multiresponsive actuators based on the conductive polymer polypyrrole.^[186,187] Additionally, thick bimorph structures (with high transmission in the NIR) achieved high-force output owing to the use of rare earth oxides^[188] or MoO_2 ^[189] as photothermal elements.

As a step forward, 3D-printing has enabled the production of rationally designed and precisely tuned photothermal actuators based on multiphoton lithography, which allows achieving a programmed printing density with high resolution. For instance, 3D-printed hydrogel actuators composed of dynamic and static layers with low and high printing density containing Au NRs presented a sharp optomechanical response.^[190] In this line, NIR-responsive and catalytic hydrogel actuators were fabricated by 3D-printing using spinach leaf-derived thylakoid membrane (nanothylakoid) as photothermal agent featuring catalase-like property.^[191]

3.1.2. Soft Actuators Based on Thermally-Driven Phase Transitions

The other common strategy to build soft photothermal actuators is to generate a phase change in the substrate material as actuating mechanical force. In particular, thermotropic liquid crystals (LC) are an ideal choice for this application due to their softness and temperature-dependent macromolecular order. These systems can be classified into liquid crystal elastomers (LCE), liquid crystal polymers (LCP), or liquid crystal networks (LCN) depending on their macromolecular structure and physicochemical properties.^[192]

Phase transitions actuators can be also combined with a variety of photothermal agents. For example, Shi et al. developed a color-changing actuator based on a Ag nanoparticle array on a LCE substrate^[193] (Figure 8a). In their approach, Ag NPs generated the necessary heat to drive a phase change in the LCE and to produce a deflection on the structure. This deflection, in turn, modified the nanoparticle arrangement, which produced a shift in the reflected color. A different example of phase change-

driven actuation was presented by Meder et al., in which AuNPs in a liquid dispersion were encapsulated in an elastomeric matrix. In this case, the plasmonic-assisted heating evaporated the encapsulated liquid, thereby causing an increase of pressure that produced the mechanical response.^[194] Also, a 3D-printing approach was developed to fabricate light-driven actuators based on shape-memory polymers with phase transitions triggered by embedded AuNPs as photothermal agent.^[195] Fe or iron-oxide (FeO) powder was used in combination with a LCN to develop a dual optical-magnetic actuator (Figure 8b),^[196,197] which was applied to develop a mechanical gripper that could be transported and rotated by a magnet and actuated using blue light. Dyes and graphene have also been used as photothermal agents to drive phase transitions in LC.^[198] For example, a polarization-dependent actuation was achieved in LCEs doped with dichroic dyes, which presented polarized light absorption and photothermal properties, thus providing an additional degree of freedom to the light-driven structures.^[199] Another interesting approximation for light-driven actuation with dye-doped LCN was presented by Zeng et al., in which a self-regulating artificial iris capable to modulate the light transmission depending on the incident light intensity was developed.^[13] The artificial iris consisted on a circular arrangement of 12 actuators composed of a LCN matrix mixed with a red dye, which was actuated by circularly polarized light to achieve the radial actuation. In addition, a core-shell fiber actuator made of LCE coated with CNTs was demonstrated as a high-force artificial muscle able to lift loads 4600-fold heavier than its own weight (Figure 8c).^[200]

3.1.3. Soft Optomechanical Actuators Based on Other Mechanisms

Analogously to the thermal expansion driven actuators, bilayer mechanical structures can be actuated by thermal dehydration. In this case, the bending mechanism is driven by a differential expansion/contraction between the two layers due the absorption/desorption of the ambient humidity triggered by light. As previously mentioned, it is possible to combine both effects (thermal expansion and thermal hydration) to produce an enhanced effect or a dual response.^[166,168] Nonetheless, soft actuators only driven by thermal dehydration have been also developed. For example, a GO-PDA actuator was developed to build origami self-folding devices^[201] (Figure 8d). Using this approach, programmable structures such as a soft-robotic hand or a walker robot were demonstrated. In this line, Arazoe et al. built an autonomous actuator with high sensitivity and extremely fast response to variations in environmental humidity.^[202] Their structures were based on π -stacked carbon nitride polymer (CNP) on a glass substrate of guanidinium carbonate (Gdm_2CO_3).

By using photothermally-controlled swelling of single layer systems, Mourran et al. studied soft, light-triggered microswimmers based on AuNPs in a PNIPAM matrix.^[204] They studied different geometries to maximize the propelling motion of the soft-robot due to the swelling/shrinking of the structure produced by the rapid photogenerated heating of AuNPs upon NIR irradiation. Lastly, a peculiar example of photothermal mediated actuation was demonstrated by Li et al.^[205] In this work, they build a magnetically-responsive actuator based on CrO_2

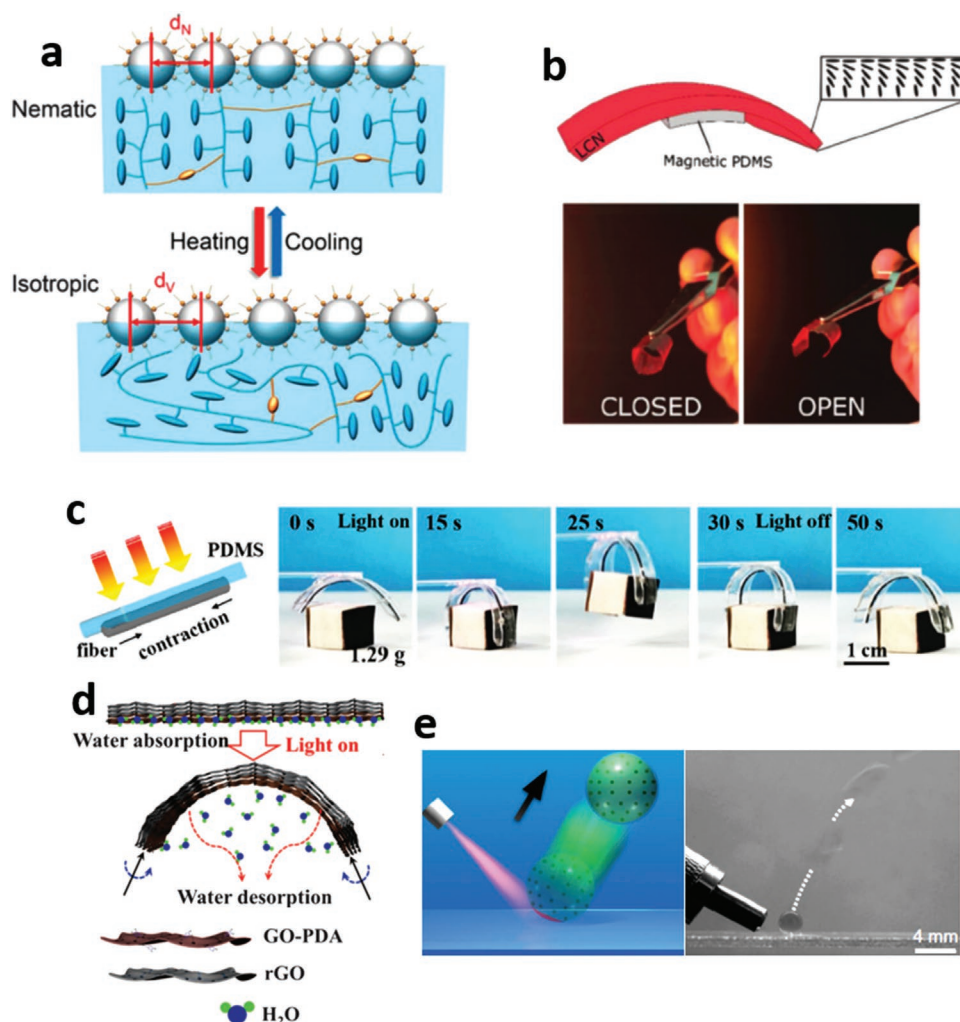


Figure 8. Soft actuators based on photothermally driven phase transitions and other mechanisms. a) Soft actuator structure based on a Ag nanoparticle array on a LCE, in which the photogenerated heat produces a phase change on the polymer and a change on the interparticle distance. Reproduced with permission.^[193] Copyright 2016, Royal Society of Chemistry. b) Iron powder-PDMS/LCN actuator providing magnetic- and light-driven actuation. Reproduced with permission.^[197] Copyright 2019, Wiley VCH-GmbH. c) Light-driven core-shell fiber actuator based on CNTs/LCE for artificial muscle and phototropic locomotion. Reproduced with permission.^[200] Copyright 2022, Elsevier. d) GO-PDA actuator based on a differential water desorption. Reproduced with permission.^[201] Copyright 2015, American Association for the Advancement of Science. e) Photogenerated air bubble actuation in hydrogel beads containing Fe_3O_4 NPs. Reproduced with permission.^[203] Copyright 2020, Springer Nature.

on PDMS and silk fibroin. Since the magnetization of CrO_2 is temperature dependent, the strength of the magnetic actuation could be controlled by the photogenerated heat.

Additionally, soft photothermal actuators based on fundamentally different actuation mechanisms than the ones described previously have been reported in the last years. For instance, Li et al. built a hydrogel actuator containing Fe_3O_4 NPs that displayed a strong and ultrafast response. In this case, the driving force was induced by the bubbles generated due to the photothermal effect while taking also advantage of the high elasticity of the hydrogel^[203] (Figure 8e). In another example, NIR and UV-responsive dye-loaded polyethylene actuators displayed fast locomotion in liquid environment thanks to a photothermally induced Marangoni effect.^[206] On the other hand, remarkable advances in light-driven microrobots based on shape-memory alloys have been also reported.^[207–209]

3.2. Soft Photochemical Actuators

Photochemical actuators rely on the conversion of light into mechanical work by the rearrangement of dynamic chemical bonds in the chemical structure of the actuator material. The endpoint macroscopic deformation depends on the collective structural reorganization at the molecular scale. The most common strategy is to include molecular photo-switches (such as azobenzenes,^[210] spiropyrans^[211] or fulgides) into the polymer-based actuator (usually composed of LCNs or LCEs). Azobenzene and its derivatives have the ability to produce a *cis-trans* isomerization as a response to a certain light wavelength (usually UV light at 365 nm), and have been widely employed to build light-controlled actuators. For example, Lamsaard et al. demonstrated the incorporation of azobenzene molecular switches into LCNs to build optomechanical devices

that support different deformations, from left-handed to right-handed helix twisting, depending on the molecular alignment with respect to the actuator geometry.^[212] Other authors followed the same principle to develop different devices, such as crawling and swimming soft microrobots^[213,214] (Figure 9a), an artificial flytrap^[10] or a biomimetic artificial cilia for lab-on-a-chip applications.^[215] Besides, other photo-switches were incorporated in order to utilize longer wavelengths compatible with biological applications. For instance, azotolane-containing LCPs driven by blue-light and natural sunlight were demonstrated.^[216,217] Additionally, Yu et al. achieved red-light and even NIR triggered actuators by including photo-luminescent compounds in addition to the azo derivatives into the polymer network.^[218,219] In these cases, the emission spectra of the luminescent dyes overlapped with the absorption band of the azotolane moieties. In addition, by combining two different photo-sensitive moieties, dual-responsive and reprogrammable actuators controlled by different light wavelengths were reported.^[220] However, since the *cis* isomer in the azobenzene molecules is transient under dark conditions, it spontaneously reverts to the *trans* form, thus compromising the stability of the photo-induced state in the actuators. In this regard, LCN actuators based on hydrazones as photochemical switches rendered a long-lasting stability (months) of the photo-induced state.^[221] On the contrary, Gelebart et al. incorporated azobenzene derivatives with fast *cis*-to-*trans* thermal relaxation into LCs, obtaining films that experienced light-induced mechanical waves rendering directional locomotion and cargo transportation.^[222]

Another strategy that has been studied is based on new classes of cross-linked polymers that include exchangeable and reversible bonds into the structure to induce rearrangements of the cross-linking network in response to the incident light. With this approach, Ube et al. combined

poly(hydrogenmethylsiloxane) and vinyl compounds to produce LCE containing dynamic covalent bonds based on ester and hydroxy groups,^[223] as shown in Figure 9b. These structures showed reversible bending upon UV and visible light, as well as the rearrangement of the initial chemical structure by heat application. In addition, LCE with allyl sulfide functional group were synthesized by other groups to fabricate optomechanical structures with different programmable actuation modes.^[224,225] In this case, the light-to-mechanical conversion was driven by the exchange reaction between allyl sulfide groups. Other examples of reversible, dynamic chemical bonds for photochemical actuation include the use of hydrogen bonds.^[226] Moreover, the panel of photo-chemical moieties used in the construction of light-fueled actuators has been widely expanded recently to, for example, anthracene derivatives,^[227,228] diarylethene derivatives,^[229] and fulgides^[230] For a deeper insight, the reader is referred to excellent reviews on this topic.^[156,231,232]

4. Summary and Outlook

In this review, the fundamental principles, design concepts, and applications of soft optomechanical systems have been overviewed. The review covers different fundamental aspects derived from the combination of the photonic and photo-thermal response of plasmonic nanostructures, dielectric micro/nano-structures (i.e., diffraction gratings, PhCs and surface wrinkles), CNMs, and macromolecules with the mechanical properties of soft-polymers. A broad range of actuation and detection mechanisms are summarized, such as soft plasmo-mechanical systems,^[233,234] mechanochromic polymers,^[235] or structurally colored polymeric materials,^[3] and light-driven actuators,^[231,232] providing a comprehensive framework for

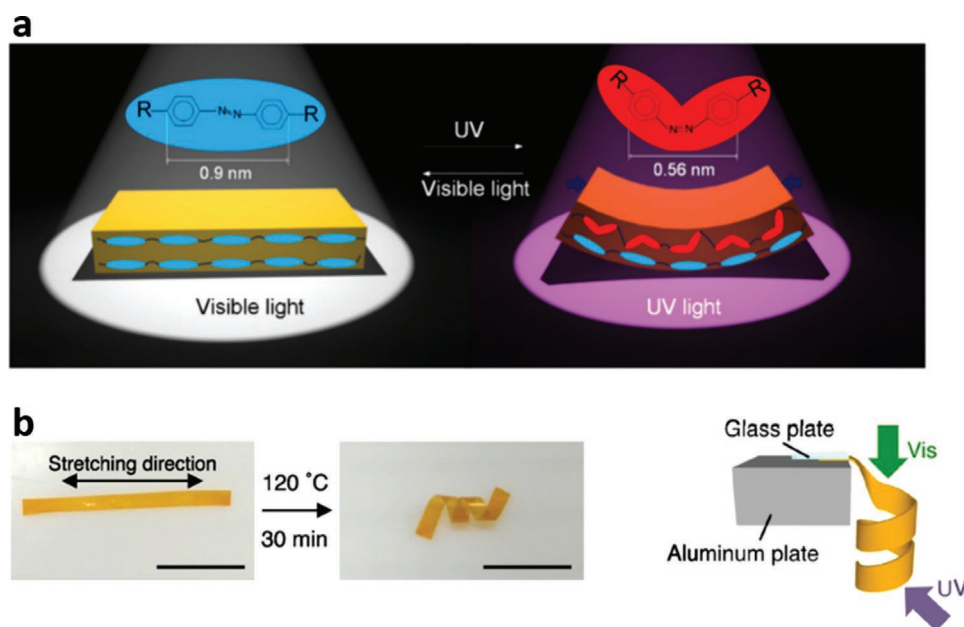


Figure 9. Soft actuators based on photochemical reactions. a) Light-mediated *cis*-*trans* isomerization of azobenzene inside an LCE matrix. Reproduced with permission.^[213] Copyright 2015, Springer Nature. b) LCE with a polysiloxane backbone displaying light-mediated sophisticated 3D motions. Reproduced with permission.^[223] Copyright 2016, Wiley-VCH Verlag GmbH & Co. KGaA.

the soft optomechanical systems and their diverse applications. In particular, the main mechanisms for applications in sensing and light modulation have been divided in i) mechanochromism generated by plasmonic features or structural coloration, and ii) changes in light intensity. On the other hand, photothermal effects and light-sensitive macromolecules are the main mechanisms of optomechanical actuation.

In contrast with conventional (hard) optomechanical devices, which are often based on high aspect-ratio micro/nanostructures such as resonators and FP cavities made of silicon or metals,^[236,237] the introduction of soft materials (Young's modulus (E) ranging between 10^4 – 10^9 Pa) offers various beneficial features. First, owing to their low stiffness and high optical transparency, soft polymers allow the use of thicker structures and even bulk materials while keeping a suitable optomechanical sensitivity, thus reducing the fabrication complexity and costs. Remarkably, soft polymer-based optomechanical systems can often be manufactured via inexpensive versatile routes that can be easily tailored to incorporate diverse functionalities. Besides, due to their excellent mechanical tunability, in most cases the optomechanical readout/stimulation can be performed with white light instead of a coherent light source. Moreover, flexible materials can adaptively fit onto curved surfaces and therefore can be utilized in, for example, wearable sensors. Despite all these advantages, hard systems are still paramount in high-precision measurements demanding outstanding sensitivity and modulation speed, e.g., mass sensing, accelerometry, ultrasound sensing, and quantum techniques.^[238–240]

Soft optomechanical materials for sensing and modulation are mainly achieved by combining plasmonic and photonic nanostructures with soft elastic materials (e.g., PDMS). Au and Fe are especially interesting materials for these applications due to their optical and thermo-plasmonic properties, while polystyrene microparticles are intensively used for the development of colloidal PhCs. In addition to self-assembly, lithography-based techniques are specially used for the fabrication of 2D features arrays when a superior control over the dimensions and positions are required. Mechanochromicity is one of the mechanisms more extensively exploited detection mechanisms, in which the material color change is measured by spectrometry or simply by visual inspection. However, the practical applications of visual color changing materials still presents some challenges related to sensitivity, detection limit, speed of response, or sensing range. Sensing applications based on polymer thermal expansion or swelling present also problems related to the time response and the relaxation time.

Measuring physical forces (strain, pressure) has been the primary focus in soft optomechanical sensors, for applications in colorimetric structural health monitoring and pressure sensing. In this line, mechanochromic systems with outstanding mechanical sensitivities and resilience have been demonstrated, which hold great potential to be translated into useful market products.^[241] On the other hand, soft mechanochromic materials have gained increasing attention in chemical and biochemical sensing.^[2] Combining the high sensitivity and biocompatibility of soft mechanical structures with the ease of use of colorimetric analysis may open unprecedented possibilities in clinical diagnostics and environmental monitoring. It is

worth mentioning that color imaging-based readouts enable 2D-mapping of the mechanical deformations and hence allow monitoring a large number of sensors in parallel. In this way, soft mechanochromic systems are also appealing as a tool for measuring the forces exerted by living cells and performing mechanobiology studies.^[242,243] In addition, integration of the soft mechanochromic materials (e.g., hydrogels) within microfluidics^[244] and paper-based devices^[245] may in turn foster new relevant applications.

Soft optomechanical modulators, mainly based on wrinkled PDMS surfaces, have been widely exploited to build high-performance smart windows and optical displays switched by external strain.^[7] These systems offer very promising features toward robust and energy-efficient solutions for future sustainable buildings. Interestingly, endowing these systems with light-driven actuation capabilities may boost the development of fully autonomous and efficient light modulators. On the other hand, it is also worth mentioning that a variety of optical modulators based on hard materials switched through optical, electrical, and thermal pulses have been developed in recent years, which have demonstrated outstanding performances; for example, tunable optical metasurfaces relying on different mechanisms for applications in tunable focusing, beam steering, and holograms.^[246] Among them, chalcogenide phase-change metamaterials play a prominent role, since they can be switched by low-power electrical/optical signals with fast transition speeds.^[247–252]

Soft optomechanical actuators have experienced a big expansion during the last years, especially for applications in soft-robotics. Light actuation can be applied remotely, eliminating the necessity of wires and, consequently, reducing the complexity of soft-robots. Light actuation can also be combined with other stimuli for multifunctional applications. However, there are still many challenges to translate soft optomechanical actuators from the lab to the market. Size, strength or high-performance actuation are some of the limitations of the current developments, which are generally demonstrated by using simple suspended beams or small size grippers. As a step forward, sunlight-driven^[182] and high-force^[188] soft actuators have been demonstrated, as well as systems harnessing novel high-performance photothermal agents.^[180] Besides, other actuation mechanisms beyond photothermal and photochemical processes are being explored, which may offer very interesting features.^[203] Remarkably, soft actuators easily incorporate a self-sensing capacity (e.g., mechanochromic) to enable precise control of the actuation strength.^[186]

Another critical issue to both optomechanical sensing and actuation devices is the lack of industrial processes for scaling up the manufacturing of PDMS-based devices. PDMS is the crucial polymer used in a significant fraction of the reviewed systems. However, although there are currently well-established methods for replicating microfabricated PDMS devices, the cost is relatively high compared to other inexpensive industry-standard polymers (i.e., thermoplastics). Mass production techniques commonly used for manufacturing polymer-based devices (e.g., injection molding, rolling, hot embossing, laser cutting or micromilling) are not transferable to PDMS processing, making it difficult to translate PDMS-based systems into the market. Moreover, PDMS is a material that swells

and absorbs small molecules that can affect the sensitivity and reproducibility of the system over time, aging and losing its original properties.^[253] Alternatively, new soft polymers recently employed for manufacturing microfluidic devices present interesting mechanical features (e.g., low Young's modulus (E), $E_{\text{PDMS}} \approx 1.8$ MPa), and may be advantageous in terms of manufacturing scalability. For example, polyester elastomers ($E \approx 0.7$ MPa)^[254] and tetrafluoroethylene-propylene elastomers ($E \approx 0.8$ MPa)^[255] have been used to build soft structures by conventional molding techniques. Interestingly, thermoplastic elastomers can be processed by injection molding and hot embossing, presenting however a higher stiffness ($E \approx 34$ MPa).^[256] On the other hand, soft structures based on thiol-ene polymers ($E \approx 10$ – 30 MPa) may be obtained by photopolymerization using UV-lithography and reaction injection molding.^[257]

In conclusion, a wide variety of soft optomechanical systems are being developed exploiting the unique features enabled by the combination of soft polymers with photonic/photo-responsive materials. Although still in its infancy, these flexible engineered systems are already offering remarkable advances in sensing, modulation, and actuation. Following this trend, these technologies will most likely provide great benefits in many fields in the near future.

Acknowledgements

The authors acknowledge the financial support from grant nos. MAT2016-77391-R, PID2019-106229RB-I00, and PCIN2016-093 (M-ERA-NET) funded by MCIN/AEI/10.13039/501100011033, and grant nos. RTI2018-096786-B-I00 funded by MCIN/AEI/10.13039/501100011033 and by "ERDF A way of making Europe". The funding from Generalitat de Catalunya through the 2017-SGR-292 project is also acknowledged. ICN2 was funded by the CERCA programme/Generalitat de Catalunya. The ICN2 was supported by the SEV-2017-0706 grant funded by MCIN/AEI/10.13039/501100011033. F.P.-V. acknowledge funding from the European Union's Horizon 2020 research and innovation programme under Marie Skłodowska-Curie grant agreement no. 801342 (Tecniopring INDUSTRY) and the Government of Catalonia's Agency for Business Competitiveness (ACCIÓ) (TECSPR19-1-0021).

Conflict of Interest

The authors declare no conflict of interest.

Keywords

light-driven mechanical actuators, mechanochromic systems, optomechanical modulators, photochemical actuators, photothermal actuators, plasmomechanical systems, soft optomechanical systems

Received: November 10, 2022

Revised: December 23, 2022

Published online: January 22, 2023

[1] M. Kolbe, S. Lee, *Adv. Mater.* **2018**, *30*, 1702669.

[2] E. Inci, G. Topcu, T. Guner, M. Demirkurt, M. M. Demir, *J. Mater. Chem. C* **2020**, *8*, 12036.

- [3] J. M. Clough, C. Weder, S. Schrettl, *Macromol. Rapid Commun.* **2021**, *42*, 2000528.
- [4] G. Chen, W. Hong, *Adv. Opt. Mater.* **2020**, *8*, 2000984.
- [5] Y. Zhou, F. Fan, Y. Liu, S. Zhao, Q. Xu, S. Wang, D. Luo, Y. Long, *Nano Energy* **2021**, *90*, 106613.
- [6] W. Hong, Z. Yuan, X. Chen, *Small* **2020**, *16*, 1907626.
- [7] D. Cho, H. Chen, J. Shin, S. Jeon, *Nanophotonics* **2021**, *11*, 2737.
- [8] H. Zhao, K. O'Brien, S. Li, R. F. Shepherd, *Sci. Robot.* **2016**, *1*, 7521.
- [9] Y. Zhao, C. Xuan, X. Qian, Y. Alsaid, M. Hua, L. Jin, X. He, *Sci. Robot.* **2019**, *4*, 7112.
- [10] O. M. Wani, H. Zeng, A. Priimagi, *Nat. Commun.* **2017**, *8*, 15546.
- [11] M.-H. Li, P. Keller, *Philos. Trans. R. Soc. Math. Phys. Eng. Sci.* **2006**, *364*, 2763.
- [12] B. Han, Y.-L. Zhang, L. Zhu, Y. Li, Z.-C. Ma, Y.-Q. Liu, X.-L. Zhang, X.-W. Cao, Q.-D. Chen, C.-W. Qiu, H.-B. Sun, *Adv. Mater.* **2019**, *31*, 1806386.
- [13] H. Zeng, O. M. Wani, P. Wasylczyk, R. Kaczmarek, A. Priimagi, *Adv. Mater.* **2017**, *29*, 1701814.
- [14] F. Li, H. Hou, J. Yin, X. Jiang, *Sci. Adv.* **2018**, *4*, eaar5762.
- [15] J. Li, R. Zhang, L. Mou, M. J. de Andrade, X. Hu, K. Yu, J. Sun, T. Jia, Y. Dou, H. Chen, S. Fang, D. Qian, Z. Liu, *Adv. Funct. Mater.* **2019**, *29*, 1808995.
- [16] L. Yu, H. Yu, *ACS Appl. Mater. Interfaces* **2015**, *7*, 3834.
- [17] F. Huang, J. J. Baumberg, *Nano Lett.* **2010**, *10*, 1787.
- [18] T. Kan, K. Matsumoto, I. Shimoyama, *Nanotechnology* **2012**, *23*, 315201.
- [19] F. Laible, D. A. Gollmer, S. Dickreuter, D. P. Kern, M. Fleischer, *Nanoscale* **2018**, *10*, 14915.
- [20] S. Aksu, M. Huang, A. Artar, A. A. Yanik, S. Selvarasah, M. R. Dokmeci, H. Altug, *Adv. Mater.* **2011**, *23*, 4422.
- [21] I. M. Pryce, K. Aydin, Y. A. Kelaita, R. M. Briggs, H. A. Atwater, *Philos. Trans. R. Soc. Math. Phys. Eng. Sci.* **2011**, *369*, 3447.
- [22] I. M. Pryce, K. Aydin, Y. A. Kelaita, R. M. Briggs, H. A. Atwater, *Nano Lett.* **2010**, *10*, 4222.
- [23] J. B. Reeves, R. K. Jayne, T. J. Stark, L. K. Barrett, A. E. White, D. J. Bishop, *Nano Lett.* **2018**, *18*, 2802.
- [24] Y.-L. Chiang, C.-W. Chen, C.-H. Wang, C.-Y. Hsieh, Y.-T. Chen, H.-Y. Shih, Y.-F. Chen, *Appl. Phys. Lett.* **2010**, *96*, 041904.
- [25] X. Han, Y. Liu, Y. Yin, *Nano Lett.* **2014**, *14*, 2466.
- [26] G. Topcu, T. Guner, E. Inci, M. M. Demir, *Sens. Actuators Phys.* **2019**, *295*, 503.
- [27] M. G. Millyard, F. Min Huang, R. White, E. Spigone, J. Kivioja, J. J. Baumberg, *Appl. Phys. Lett.* **2012**, *100*, 073101.
- [28] M. A. Mahmoud, *J. Phys. Chem. C* **2015**, *119*, 19359.
- [29] A. Mizuno, A. Ono, *ACS Appl. Nano Mater.* **2021**, *4*, 9721.
- [30] D. Dong, R. Fu, Q. Shi, W. Cheng, *Nat. Protoc.* **2019**, *14*, 2691.
- [31] R. Fu, T. Warnakula, Q. Shi, L. Wei Yap, D. Dong, Y. Liu, M. Premaratne, W. Cheng, *Nanoscale Horiz.* **2020**, *5*, 1515.
- [32] R. Fu, D. E. Gómez, Q. Shi, L. W. Yap, Q. Lyu, K. Wang, Z. Yong, W. Cheng, *Nano Lett.* **2021**, *21*, 389.
- [33] U. Cataldi, P. Cerminara, L. D. Sio, R. Caputo, C. P. Umeton, *Mol. Cryst. Liq. Cryst.* **2012**, *558*, 22.
- [34] U. Cataldi, R. Caputo, Y. Kurylyak, G. Klein, M. Chekini, C. Umeton, T. Bürgi, *J. Mater. Chem. C* **2014**, *2*, 7927.
- [35] R. Caputo, U. Cataldi, T. Bürgi, C. Umeton, *Mol. Cryst. Liq. Cryst.* **2015**, *614*, 20.
- [36] T. Maurer, J. Marae-Djouda, U. Cataldi, A. Gontier, G. Montay, Y. Madi, B. Panicaud, D. Macias, P.-M. Adam, G. Lévêque, T. Bürgi, R. Caputo, *Front. Mater. Sci.* **2015**, *9*, 170.
- [37] G. Palermo, U. Cataldi, A. Condello, R. Caputo, T. Bürgi, C. Umeton, A. D. Luca, *Nanoscale* **2018**, *10*, 16556.
- [38] Y. Cui, J. Zhou, V. A. Tamma, W. Park, *ACS Nano* **2012**, *6*, 2385.
- [39] L. Gao, Y. Zhang, H. Zhang, S. Doshay, X. Xie, H. Luo, D. Shah, Y. Shi, S. Xu, H. Fang, J. A. Fan, P. Nordlander, Y. Huang, J. A. Rogers, *ACS Nano* **2015**, *9*, 5968.

- [40] C. A. S. Burel, A. Alsayed, L. Malassis, C. B. Murray, B. Donnio, R. Dreyfus, *Small* **2017**, 13, 1701925.
- [41] O. Eskilson, S. B. Lindström, B. Sepulveda, M. M. Shahjamali, P. Güell-Grau, P. Sivilér, M. Skog, C. Aronsson, E. M. Björk, N. Nyberg, H. Khalaf, T. Bengtsson, J. James, M. B. Ericson, E. Martinsson, R. Selegård, D. Aili, *Adv. Funct. Mater.* **2020**, 30, 2004766.
- [42] A. Choe, J. Yeom, R. Shanker, M. P. Kim, S. Kang, H. Ko, *NPG Asia Mater* **2018**, 10, 912.
- [43] M. Nuopponen, H. Tenhu, *Langmuir* **2007**, 23, 5352.
- [44] P. Wang, L. Zhang, Y. Xia, L. Tong, X. Xu, Y. Ying, *Nano Lett.* **2012**, 12, 3145.
- [45] R. M. Cole, S. Mahajan, J. J. Baumberg, *Appl. Phys. Lett.* **2009**, 95, 154103.
- [46] X. Zhu, L. Shi, X. Liu, J. Zi, Z. Wang, *Nano Res.* **2010**, 3, 807.
- [47] X. Zhu, S. Xiao, L. Shi, X. Liu, J. Zi, O. Hansen, N. A. Mortensen, *Opt. Express* **2012**, 20, 5237.
- [48] X. Zhang, J. Zhang, H. Liu, X. Su, L. Wang, *Sci. Rep.* **2014**, 4, 4182.
- [49] F. Lütolf, D. Casari, B. Gallinet, *Adv. Opt. Mater.* **2016**, 4, 715.
- [50] D. Yoo, T. W. Johnson, S. Cherukulappurath, D. J. Norris, S.-H. Oh, *ACS Nano* **2015**, 9, 10647.
- [51] W. Chen, W. Liu, Y. Jiang, M. Zhang, N. Song, N. J. Greybush, J. Guo, A. K. Estep, K. T. Turner, R. Agarwal, C. R. Kagan, *ACS Nano* **2018**, 12, 10683.
- [52] L. Xu, Y. Feng, D. Yu, Z. Zheng, X. Chen, W. Hong, *Adv. Mater. Technol.* **2020**, 5, 2000373.
- [53] P. Güell-Grau, F. Pi, R. Villa, O. Eskilson, D. Aili, J. Nogués, B. Sepúlveda, M. Alvarez, *Adv. Mater.* **2022**, 34, 2106731.
- [54] G. Bae, M. Seo, S. Lee, D. Bae, M. Lee, *Adv. Mater. Technol.* **2021**, 6, 2100118.
- [55] S. Kinoshita, S. Yoshioka, J. Miyazaki, *Rep. Prog. Phys.* **2008**, 71, 076401.
- [56] L. J. Guo, *Adv. Mater.* **2007**, 19, 495.
- [57] N. Kooy, K. Mohamed, L. T. Pin, O. S. Guan, *Nanoscale Res. Lett.* **2014**, 9, 320.
- [58] T. Karrock, M. Gerken, *Biomed. Opt. Express* **2015**, 6, 4901.
- [59] Y. Nazirizadeh, T. Karrock, M. Gerken, *Opt. Lett.* **2012**, 37, 3081.
- [60] R. Zhang, Z. Yang, X. Zheng, Y. Zhang, Q. Wang, *J. Mater. Sci. Mater. Electron.* **2021**, 32, 15586.
- [61] K. Suzumori, M. Mihara, S. Wakimoto, in *2011 IEEE International Conference on Robotics and Automation*, **2011**, 2771.
- [62] Y. Zhu, M. Xu, H. Jin, J. Yang, E. Dong, in *2017 IEEE International Conference on Robotics and Automation (ICRA)*, **2017**, 6737.
- [63] P. Güell-Grau, P. Escudero, F. G. Perdikos, J. F. López-Barbera, C. Pascual-Izarra, R. Villa, J. Nogués, B. Sepúlveda, M. Alvarez, *ACS Appl. Mater. Interfaces* **2021**, 13, 47871.
- [64] F. Pujol-Vila, P. Escudero, P. Güell-Grau, C. Pascual-Izarra, R. Villa, M. Alvarez, *Small Methods* **2022**, 6, 2101283.
- [65] Y.-J. Quan, Y.-G. Kim, M.-S. Kim, S.-H. Min, S.-H. Ahn, *ACS Nano* **2020**, 14, 5392.
- [66] P. Escudero, J. Yeste, C. Pascual-Izarra, R. Villa, M. Alvarez, *Sci. Rep.* **2019**, 9, 3259.
- [67] C.-M. Chen, S. Yang, *Polym. Int.* **2012**, 61, 1041.
- [68] Z. Li, Y. Liu, M. Marin, Y. Yin, *Nano Res.* **2020**, 13, 1882.
- [69] K. Wu, T. Zhu, L. Zhu, Y. Sun, K. Chen, J. Chen, H. Yuan, Y. Wang, J. Zhang, G. Liu, X. Chen, J. Sun, *Nano Lett.* **2022**, 22, 2261.
- [70] Y. Qi, C. Zhou, S. Zhang, Z. Zhang, W. Niu, S. Wu, W. Ma, B. Tang, *Dyes Pigments* **2021**, 189, 109264.
- [71] H. Xu, C. Yu, S. Wang, V. Malyarchuk, T. Xie, J. A. Rogers, *Adv. Funct. Mater.* **2013**, 23, 3299.
- [72] M. L. Tseng, J. Yang, M. Semmlinger, C. Zhang, P. Nordlander, N. J. Halas, *Nano Lett.* **2017**, 17, 6034.
- [73] Y. Wang, L. Liu, Q. Wang, W. Han, M. Lu, L. Dong, *Appl. Phys. Lett.* **2016**, 108, 071110.
- [74] C. López, *Adv. Mater.* **2003**, 15, 1679.
- [75] R. Zhang, Q. Wang, X. Zheng, *J. Mater. Chem. C* **2018**, 6, 3182.
- [76] I. R. Howell, C. Li, N. S. Colella, K. Ito, J. J. Watkins, *ACS Appl. Mater. Interfaces* **2015**, 7, 3641.
- [77] T.-W. Lu, C.-C. Wu, P.-T. Lee, *ACS Photonics* **2018**, 5, 2767.
- [78] P. Zhao, B. Li, Z. Tang, Y. Gao, H. Tian, H. Chen, *Smart Mater. Struct.* **2019**, 28, 075037.
- [79] H. Fudouzi, Y. Xia, *Adv. Mater.* **2003**, 15, 892.
- [80] N. Vogel, S. Goerres, K. Landfester, C. K. Weiss, *Macromol. Chem. Phys.* **2011**, 212, 1719.
- [81] J. M. Weissman, H. B. Sunkara, A. S. Tse, S. A. Asher, *Science* **1996**, 274, 959.
- [82] H. Fudouzi, Y. Xia, *Langmuir* **2003**, 19, 9653.
- [83] H. Fudouzi, T. Sawada, *Langmuir* **2006**, 22, 1365.
- [84] A. Kontogeorgos, D. R. E. Snoswell, C. E. Finlayson, J. J. Baumberg, P. Spahn, G. P. Hellmann, *Phys. Rev. Lett.* **2010**, 105, 233909.
- [85] B. Viel, T. Ruhl, G. P. Hellmann, *Chem. Mater.* **2007**, 19, 5673.
- [86] A. K. Yetisen, H. Butt, L. R. Volpatti, I. Pavlichenko, M. Humar, S. J. J. Kwok, H. Koo, K. S. Kim, I. Naydenova, A. Khademhosseini, S. K. Hahn, S. H. Yun, *Biotechnol. Adv.* **2016**, 34, 250.
- [87] Y. Fang, Y. Ni, S.-Y. Leo, C. Taylor, V. Basile, P. Jiang, *Nat. Commun.* **2015**, 6, 7416.
- [88] E. Miwa, K. Watanabe, F. Asai, T. Seki, K. Urayama, J. Odent, J.-M. Raquez, Y. Takeoka, *ACS Appl. Polym. Mater.* **2020**, 2, 4078.
- [89] E. Inci, G. Topcu, M. M. Demir, *Sens. Actuators, B* **2020**, 305, 127452.
- [90] C.-H. Cheng, S. Masuda, S. Nozaki, C. Nagano, T. Hirai, K. Kojio, A. Takahara, *Macromolecules* **2020**, 53, 4541.
- [91] D. Yang, S. Ye, J. Ge, *Adv. Funct. Mater.* **2014**, 24, 3197.
- [92] G. H. Lee, S. H. Han, J. B. Kim, D. J. Kim, S. Lee, W. M. Hamonangan, J. M. Lee, S.-H. Kim, *ACS Appl. Polym. Mater.* **2020**, 2, 706.
- [93] L. Li, Z. Chen, C. Shao, L. Sun, L. Sun, Y. Zhao, *Adv. Funct. Mater.* **2020**, 30, 1906353.
- [94] I. Jurewicz, A. A. K. King, R. Shanker, M. J. Large, R. J. Smith, R. Maspero, S. P. Ogilvie, J. Scheerder, J. Han, C. Backes, J. M. Razal, M. Florescu, J. L. Keddie, J. N. Coleman, A. B. Dalton, *Adv. Funct. Mater.* **2020**, 30, 2002473.
- [95] A. C. Arsenault, T. J. Clark, G. von Freymann, L. Cademartiri, R. Sapienza, J. Bertolotti, E. Vekris, S. Wong, V. Kitaev, I. Manners, R. Z. Wang, S. John, D. Wiersma, G. A. Ozin, *Nat. Mater.* **2006**, 5, 179.
- [96] K. Matsubara, M. Watanabe, Y. Takeoka, *Angew. Chem., Int. Ed.* **2007**, 46, 1688.
- [97] I. B. Burgess, M. Lončar, J. Aizenberg, *J. Mater. Chem. C* **2013**, 1, 6075.
- [98] C. Zhu, W. Xu, L. Chen, W. Zhang, H. Xu, Z.-Z. Gu, *Adv. Funct. Mater.* **2011**, 21, 2043.
- [99] J. Kim, S.-E. Choi, H. Lee, S. Kwon, *Adv. Mater.* **2013**, 25, 1415.
- [100] L. Shang, W. Zhang, K. Xu, Y. Zhao, *Mater. Horiz* **2019**, 6, 945.
- [101] X. Fei, T. Lu, J. Ma, W. Wang, S. Zhu, D. Zhang, *ACS Appl. Mater. Interfaces* **2016**, 8, 27091.
- [102] W. Luo, Q. Cui, K. Fang, K. Chen, H. Ma, J. Guan, *Nano Lett.* **2020**, 20, 803.
- [103] X. Hong, Y. Peng, J. Bai, B. Ning, Y. Liu, Z. Zhou, Z. Gao, *Small* **2014**, 10, 1308.
- [104] F. Xue, Z. Meng, F. Wang, Q. Wang, M. Xue, Z. Xu, *J. Mater. Chem. A* **2014**, 2, 9559.
- [105] C. Zhang, G. G. Cano, P. V. Braun, *Adv. Mater.* **2014**, 26, 5678.
- [106] Z. Cai, A. Sasmal, X. Liu, S. A. Asher, *ACS Sens.* **2017**, 2, 1474.
- [107] M. Qin, M. Sun, M. Hua, X. He, *Curr. Opin. Solid State Mater. Sci.* **2019**, 23, 13.
- [108] M. Qin, M. Sun, R. Bai, Y. Mao, X. Qian, D. Sikka, Y. Zhao, H. J. Qi, Z. Suo, X. He, *Adv. Mater.* **2018**, 30, 1800468.
- [109] F. Zhang, Q. Shen, X. Shi, S. Li, W. Wang, Z. Luo, G. He, P. Zhang, P. Tao, C. Song, W. Zhang, D. Zhang, T. Deng, W. Shang, *Adv. Mater.* **2015**, 27, 1077.

- [110] T. S. Kustandi, H. Y. Low, J. H. Teng, I. Rodriguez, R. Yin, *Small* **2009**, *5*, 574.
- [111] A. D. Pris, Y. Utturkar, C. Surman, W. G. Morris, A. Vert, S. Zalyubovskiy, T. Deng, H. T. Ghiradella, R. A. Potyrailo, *Nat. Photonics* **2012**, *6*, 195.
- [112] T. Lu, H. Pan, J. Ma, Y. Li, S. Zhu, D. Zhang, *ACS Appl. Mater. Interfaces* **2017**, *9*, 34279.
- [113] Y. Yue, T. Kurokawa, M. A. Haque, T. Nakajima, T. Nonoyama, X. Li, I. Kajiwara, J. P. Gong, *Nat. Commun.* **2014**, *5*, 4659.
- [114] Md. A. Haque, T. Kurokawa, G. Kamita, Y. Yue, J. P. Gong, *Chem. Mater.* **2011**, *23*, 5200.
- [115] M. Kolle, A. Lethbridge, M. Kreysing, J. J. Baumberg, J. Aizenberg, P. Vukusic, *Adv. Mater.* **2013**, *25*, 2239.
- [116] P. Wu, J. Wang, L. Jiang, *Mater. Horiz* **2020**, *7*, 338.
- [117] Y. Wu, Y. Wang, S. Zhang, S. Wu, *ACS Nano* **2021**, *15*, 15720.
- [118] A. E. Schedl, I. Howell, J. J. Watkins, H.-W. Schmidt, *Macromol. Rapid Commun.* **2020**, *41*, 2000069.
- [119] J. M. Clough, J. van der Gucht, T. E. Kodger, J. Sprakel, *Adv. Funct. Mater.* **2020**, *30*, 2002716.
- [120] P. Shi, E. Miwa, J. He, M. Sakai, T. Seki, Y. Takeoka, *ACS Appl. Mater. Interfaces* **2021**, *13*, 55591.
- [121] Y. Wang, L. Shang, G. Chen, L. Sun, X. Zhang, Y. Zhao, *Sci. Adv.* **2020**, *6*, eaax8258.
- [122] F. Fu, L. Shang, Z. Chen, Y. Yu, Y. Zhao, *Sci. Robot.* **2018**, *3*, eaar8580.
- [123] L. Sun, Z. Chen, F. Bian, Y. Zhao, *Adv. Funct. Mater.* **2020**, *30*, 1907820.
- [124] A. Ryabchun, A. Bobrovsky, *Adv. Opt. Mater.* **2018**, *6*, 1800335.
- [125] R. Kizhakidathazhath, Y. Geng, V. S. R. Jampani, C. Charni, A. Sharma, J. P. F. Lagerwall, *Adv. Funct. Mater.* **2020**, *30*, 1909537.
- [126] A. Tran, C. E. Boott, M. J. MacLachlan, *Adv. Mater.* **2020**, *32*, 1905876.
- [127] E. P. A. van Heeswijk, L. Yang, N. Grossiord, A. P. H. J. Schenning, *Adv. Funct. Mater.* **2020**, *30*, 1906833.
- [128] C. E. Boott, A. Tran, W. Y. Hamad, M. J. MacLachlan, *Angew. Chem., Int. Ed.* **2020**, *59*, 226.
- [129] S. Hussain, S. Park, *ACS Appl. Mater. Interfaces* **2021**, *13*, 59275.
- [130] C. Yang, B. Wu, J. Ruan, P. Zhao, J. Shan, R. Zhang, D. K. Yoon, D. Chen, K. Liu, *ACS Appl. Polym. Mater.* **2022**, *4*, 463.
- [131] A. Belmonte, M. Pilz da Cunha, K. Nickmans, A. P. H. J. Schenning, *Adv. Opt. Mater.* **2020**, *8*, 2000054.
- [132] A. M. Martinez, M. K. McBride, T. J. White, C. N. Bowman, *Adv. Funct. Mater.* **2020**, *30*, 2003150.
- [133] P. Zhang, X. Shi, A. P. H. J. Schenning, G. Zhou, L. T. de Haan, *Adv. Mater. Interfaces* **2020**, *7*, 1901878.
- [134] C. H. Barty-King, C. L. C. Chan, R. M. Parker, M. M. Bay, R. Vadrucchi, M. De Volder, S. Vignolini, *Adv. Mater.* **2021**, *33*, 2102112.
- [135] Y. Geng, R. Kizhakidathazhath, J. P. F. Lagerwall, *Nat. Mater.* **2022**, *21*, 1441.
- [136] M. Feng, X. Bu, J. Yang, D. Li, Z. Zhang, Y. Dai, X. Zhang, *J. Mater. Sci.* **2020**, *55*, 8444.
- [137] P. Kim, Y. Hu, J. Alvarenga, M. Kolle, Z. Suo, J. Aizenberg, *Adv. Opt. Mater.* **2013**, *1*, 381.
- [138] M. Shrestha, G.-K. Lau, *Opt. Lett.* **2016**, *41*, 4433.
- [139] Y. Wang, Y. Zhai, A. Villada, S. N. David, X. Yin, J. Xiao, *Appl. Phys. Lett.* **2018**, *112*, 251603.
- [140] Y. Wang, A. Villada, Y. Zhai, Z. Zou, Y. Chen, X. Yin, J. Xiao, *Appl. Phys. Lett.* **2019**, *114*, 193701.
- [141] Z. Li, Y. Zhai, Y. Wang, G. M. Wendland, X. Yin, J. Xiao, *Adv. Opt. Mater.* **2017**, *5*, 1700425.
- [142] B. Jiang, L. Liu, Z. Gao, Z. Feng, Y. Zheng, W. Wang, *ACS Appl. Mater. Interfaces* **2019**, *11*, 40406.
- [143] S. Zeng, R. Li, S. G. Freire, V. M. M. Garbellotto, E. Y. Huang, A. T. Smith, C. Hu, W. R. T. Tait, Z. Bian, G. Zheng, D. Zhang, L. Sun, *Adv. Mater.* **2017**, *29*, 1700828.
- [144] S. G. Lee, D. Y. Lee, H. S. Lim, D. H. Lee, S. Lee, K. Cho, *Adv. Mater.* **2010**, *22*, 5013.
- [145] G. Lin, P. Chandrasekaran, C. Lv, Q. Zhang, Y. Tang, L. Han, J. Yin, *ACS Appl. Mater. Interfaces* **2017**, *9*, 26510.
- [146] Q. Zhou, J. G. Park, J. Bae, D. Ha, J. Park, K. Song, T. Kim, *Adv. Mater.* **2020**, *32*, 2001467.
- [147] A. Oyefusi, J. Chen, *Appl. Mater. Today* **2020**, *20*, 100774.
- [148] Z. Mao, S. Zeng, K. Shen, A. P. Chooi, A. T. Smith, M. D. Jones, Y. Zhou, X. Liu, L. Sun, *Adv. Opt. Mater.* **2020**, *8*, 2001472.
- [149] H. Chen, D. Cho, K. Ko, C. Qin, M. P. Kim, H. Zhang, J.-H. Lee, E. Kim, D. Park, X. Shen, J. Yang, H. Ko, J.-W. Hong, J.-K. Kim, S. Jeon, *ACS Nano* **2022**, *16*, 68.
- [150] M. Barelli, D. Repetto, F. B. de Mongeot, *ACS Appl. Polym. Mater.* **2019**, *1*, 1334.
- [151] G. Stoychev, A. Kirillova, L. Ionov, *Adv. Opt. Mater.* **2019**, *7*, 1900067.
- [152] M. Mauro, *J. Mater. Chem. B* **2019**, *7*, 4234.
- [153] H. K. Bisoyi, A. M. Urbas, Q. Li, *Adv. Opt. Mater.* **2018**, *6*, 1800458.
- [154] B. Han, Y.-L. Zhang, Q.-D. Chen, H.-B. Sun, *Adv. Funct. Mater.* **2018**, *28*, 1802235.
- [155] X.-L. Weng, J.-Y. Liu, *Drug Discov. Today* **2021**, *26*, 2045.
- [156] J. Li, X. Zhou, Z. Liu, *Adv. Opt. Mater.* **2020**, *8*, 2000886.
- [157] D. Yoon, Y.-W. Son, H. Cheong, *Nano Lett.* **2011**, *11*, 3227.
- [158] Q. Shi, H. Xia, P. Li, Y.-S. Wang, L. Wang, S.-X. Li, G. Wang, C. Lv, L.-G. Niu, H.-B. Sun, *Adv. Opt. Mater.* **2017**, *5*, 1700442.
- [159] J. Chen, J. Feng, F. Yang, R. Aleisa, Q. Zhang, Y. Yin, *Angew. Chem., Int. Ed.* **2019**, *58*, 9275.
- [160] P. Güell-Grau, F. Pi, R. Villa, J. Nogués, M. Alvarez, B. Sepúlveda, *Appl. Mater. Today* **2021**, *23*, 101052.
- [161] Z. Li, Z. Ye, L. Han, Q. Fan, C. Wu, D. Ding, H. L. Xin, N. V. Myung, Y. Yin, *Adv. Mater.* **2021**, *33*, 2006367.
- [162] Y. Hu, G. Wu, T. Lan, J. Zhao, Y. Liu, W. Chen, *Adv. Mater.* **2015**, *27*, 7867.
- [163] X. Wang, N. Jiao, S. Tung, L. Liu, *ACS Appl. Mater. Interfaces* **2019**, *11*, 30290.
- [164] Leeladhar, P. Raturi, J. P. Singh, *Sci. Rep.* **2018**, *8*, 3687.
- [165] D. Gao, M.-F. Lin, J. Xiong, S. Li, S. N. Lou, Y. Liu, J.-H. Ciou, X. Zhou, P. S. Lee, *Nanoscale Horiz.* **2020**, *5*, 730.
- [166] Y.-Y. Gao, Y.-L. Zhang, B. Han, L. Zhu, B. Dong, H.-B. Sun, *ACS Appl. Mater. Interfaces* **2019**, *11*, 37130.
- [167] Y. Yang, Y. Liu, Y. Shen, *Adv. Funct. Mater.* **2020**, *30*, 1910172.
- [168] Y.-L. Zhang, J.-N. Ma, S. Liu, D.-D. Han, Y.-Q. Liu, Z.-D. Chen, J.-W. Mao, H.-B. Sun, *Nano Energy* **2020**, *68*, 104302.
- [169] H. Luo, Y. Lu, J. Qiu, *ACS Appl. Mater. Interfaces* **2021**, *13*, 32046.
- [170] W. Wang, C. Xiang, Q. Zhu, W. Zhong, M. Li, K. Yan, D. Wang, *ACS Appl. Mater. Interfaces* **2018**, *10*, 27215.
- [171] Y. Yamamoto, K. Kanao, T. Arie, S. Akita, K. Takei, *ACS Appl. Mater. Interfaces* **2015**, *7*, 11002.
- [172] Y. Hu, J. Liu, L. Chang, L. Yang, A. Xu, K. Qi, P. Lu, G. Wu, W. Chen, Y. Wu, *Adv. Funct. Mater.* **2017**, *27*, 1704388.
- [173] X. Zhang, Z. Yu, C. Wang, D. Zarrouk, J.-W. T. Seo, J. C. Cheng, A. D. Buchan, K. Takei, Y. Zhao, J. W. Ager, J. Zhang, M. Hettick, M. C. Hersam, A. P. Pisano, R. S. Fearing, A. Javey, *Nat. Commun.* **2014**, *5*, 2983.
- [174] L. Yang, L. Chang, Y. Hu, M. Huang, Q. Ji, P. Lu, J. Liu, W. Chen, Y. Wu, *Adv. Funct. Mater.* **2020**, *30*, 1908842.
- [175] H. Lim, T. Park, J. Na, C. Park, B. Kim, E. Kim, *NPG Asia Mater.* **2017**, *9*, e399.
- [176] G. Cai, J.-H. Ciou, Y. Liu, Y. Jiang, P. S. Lee, *Sci. Adv.* **2019**, *5*, eaaw7956.
- [177] Z. Sun, C. Song, J. Zhou, C. Hao, W. Liu, H. Liu, J. Wang, M. Huang, S. He, M. Yang, *Macromol. Rapid Commun.* **2021**, *42*, 2100499.
- [178] S. Zavahir, P. Sobolčiak, I. Krupa, D. S. Han, J. Tkac, P. Kasak, *Nanomaterials* **2020**, *10*, 1419.

- [179] S. Tu, L. Xu, J. K. El-Demellawi, H. Liang, X. Xu, S. Lopatin, S. De Wolf, X. Zhang, H. N. Alshareef, *Nano Energy* **2020**, *77*, 105277.
- [180] V. H. Nguyen, R. Tabassian, S. Oh, S. Nam, M. Mahato, P. Thangasamy, A. Rajabi-Abhari, W.-J. Hwang, A. K. Taseer, I.-K. Oh, *Adv. Funct. Mater.* **2020**, *30*, 1909504.
- [181] X.-J. Luo, L. Li, H.-B. Zhang, S. Zhao, Y. Zhang, W. Chen, Z.-Z. Yu, *ACS Appl. Mater. Interfaces* **2021**, *13*, 45833.
- [182] Y. Hu, L. Yang, Q. Yan, Q. Ji, L. Chang, C. Zhang, J. Yan, R. Wang, L. Zhang, G. Wu, J. Sun, B. Zi, W. Chen, Y. Wu, *ACS Nano* **2021**, *15*, 5294.
- [183] M. Li, L. Yuan, Y. Liu, F. Vogelbacher, X. Hou, Y. Song, Q. Cheng, *Cell Rep. Phys. Sci.* **2022**, *3*, 100915.
- [184] X. Wei, L. Chen, Y. Wang, Y. Sun, C. Ma, X. Yang, S. Jiang, G. Duan, *Chem. Eng. J.* **2022**, *433*, 134258.
- [185] M. Ha, G. S. Cañón Bermúdez, J. A.-C. Liu, E. S. Oliveros Mata, B. A. Evans, J. B. Tracy, D. Makarov, *Adv. Mater.* **2021**, *33*, 2008751.
- [186] C.-Y. Lo, Y. Zhao, C. Kim, Y. Alsaïd, R. Khodambashi, M. Peet, R. Fisher, H. Marvi, S. Berman, D. Aukes, X. He, *Mater. Today* **2021**, *50*, 35.
- [187] X. Wang, L. Li, E. Liu, J. Wang, X. Han, Y. Cao, C. Lu, *ACS Appl. Nano Mater.* **2021**, *4*, 5349.
- [188] P. Shan, X. Chen, B. Tan, D. Cao, L. Fang, C. Lu, Z. Xu, *Macromol. Mater. Eng.* **2022**, *307*, 2100683.
- [189] Z. Sun, C. Wei, W. Liu, H. Liu, J. Liu, R. Hao, M. Huang, S. He, *ACS Appl. Mater. Interfaces* **2021**, *13*, 33404.
- [190] A. Nishiguchi, H. Zhang, S. Schweizerhof, M. F. Schulte, A. Mourran, M. Möller, *ACS Appl. Mater. Interfaces* **2020**, *12*, 12176.
- [191] H. Zhao, Y. Huang, F. Lv, L. Liu, Q. Gu, S. Wang, *Adv. Funct. Mater.* **2021**, *31*, 2105544.
- [192] T. J. White, D. J. Broer, *Nat. Mater.* **2015**, *14*, 1087.
- [193] Y. Shi, C. Zhu, J. Li, J. Wei, J. Guo, *New J. Chem.* **2016**, *40*, 7311.
- [194] F. Meder, G. A. Naselli, A. Sadeghi, B. Mazzolai, *Adv. Mater.* **2019**, *31*, 1905671.
- [195] Y. Wang, E. Sachyani Keneth, A. Kamyshny, G. Scalet, F. Auricchio, S. Magdassi, *Adv. Mater. Technol.* **2021**, *7*, 2101058.
- [196] M. Pilz da Cunha, Y. Foelen, T. A. P. Engels, K. Papamichou, M. Hagenbeek, M. G. Debije, A. P. H. J. Schenning, *Adv. Opt. Mater.* **2019**, *7*, 1801604.
- [197] M. Pilz da Cunha, Y. Foelen, R. J. H. van Raak, J. N. Murphy, T. A. P. Engels, M. G. Debije, A. P. H. J. Schenning, *Adv. Opt. Mater.* **2019**, *7*, 1801643.
- [198] G. Vantomme, A. H. Gelebart, D. J. Broer, E. W. Meijer, *J. Polym. Sci. Part Polym. Chem.* **2018**, *56*, 1331.
- [199] Y. Li, Y. Liu, D. Luo, *Adv. Opt. Mater.* **2021**, *9*, 2001861.
- [200] Y. Yu, L. Li, E. Liu, X. Han, J. Wang, Y.-X. Xie, C. Lu, *Carbon* **2022**, *187*, 97.
- [201] J. Mu, C. Hou, H. Wang, Y. Li, Q. Zhang, M. Zhu, *Sci. Adv.* **2015**, *1*, 1500533.
- [202] H. Arazoe, D. Miyajima, K. Akaike, F. Araoka, E. Sato, T. Hikima, M. Kawamoto, T. Aida, *Nat. Mater.* **2016**, *15*, 1084.
- [203] M. Li, X. Wang, B. Dong, M. Sitti, *Nat. Commun.* **2020**, *11*, 3988.
- [204] A. Mourran, H. Zhang, R. Vinokur, M. Möller, *Adv. Mater.* **2017**, *29*, 1604825.
- [205] M. Li, Y. Wang, A. Chen, A. Naidu, B. S. Napier, W. Li, C. L. Rodriguez, S. A. Crooker, F. G. Omenetto, *Proc. Natl. Acad. Sci.* **2018**, *115*, 8119.
- [206] X. Pan, N. Grossiord, J. A. H. P. Sol, M. G. Debije, A. P. H. J. Schenning, *Adv. Funct. Mater.* **2021**, *31*, 2100465.
- [207] H.-T. Lee, M.-S. Kim, G.-Y. Lee, C.-S. Kim, S.-H. Ahn, *Small* **2018**, *14*, 1801023.
- [208] M.-S. Kim, H.-T. Lee, S.-H. Ahn, *Adv. Mater. Technol.* **2019**, *4*, 1900583.
- [209] Z. Shi, J. Pan, J. Tian, H. Huang, Y. Jiang, S. Zeng, *J. Bionic Eng* **2019**, *16*, 582.
- [210] X. Pang, J. Lv, C. Zhu, L. Qin, Y. Yu, *Adv. Mater.* **2019**, *31*, 1904224.
- [211] J. Keyvan Rad, Z. Balzade, A. R. Mahdavian, *J. Photochem. Photobiol. C Photochem. Rev.* **2022**, *51*, 100487.
- [212] S. Iamsaard, S. J. Aßhoff, B. Matt, T. Kudernac, J. J. L. M. Cornelissen, S. P. Fletcher, N. Katsonis, *Nat. Chem.* **2014**, *6*, 229.
- [213] C. Huang, J. Lv, X. Tian, Y. Wang, Y. Yu, J. Liu, *Sci. Rep.* **2015**, *5*, 17414.
- [214] S. Palagi, A. G. Mark, S. Y. Reigh, K. Melde, T. Qiu, H. Zeng, C. Parmeggiani, D. Martella, A. Sanchez-Castillo, N. Kapernaum, F. Giesselmann, D. S. Wiersma, E. Lauga, P. Fischer, *Nat. Mater.* **2016**, *15*, 647.
- [215] C. L. van Oosten, C. W. M. Bastiaansen, D. J. Broer, *Nat. Mater.* **2009**, *8*, 677.
- [216] F. Cheng, Y. Zhang, R. Yin, Y. Yu, *J. Mater. Chem.* **2010**, *20*, 4888.
- [217] D. Iqbal, M. H. Samiullah, *Materials* **2013**, *6*, 116.
- [218] Z. Jiang, M. Xu, F. Li, Y. Yu, *J. Am. Chem. Soc.* **2013**, *135*, 16446.
- [219] W. Wu, L. Yao, T. Yang, R. Yin, F. Li, Y. Yu, *J. Am. Chem. Soc.* **2011**, *133*, 15810.
- [220] A. H. Gelebart, D. J. Mulder, G. Vantomme, A. P. H. J. Schenning, D. J. Broer, *Angew. Chem., Int. Ed.* **2017**, *56*, 13436.
- [221] A. Ryabchun, Q. Li, F. Lancia, I. Aprahamian, N. Katsonis, *J. Am. Chem. Soc.* **2019**, *141*, 1196.
- [222] A. H. Gelebart, D. Jan Mulder, M. Varga, A. Konya, G. Vantomme, E. W. Meijer, R. L. B. Selinger, D. J. Broer, *Nature* **2017**, *546*, 632.
- [223] T. Ube, K. Kawasaki, T. Ikeda, *Adv. Mater.* **2016**, *28*, 8212.
- [224] X. Qian, Q. Chen, Y. Yang, Y. Xu, Z. Li, Z. Wang, Y. Wu, Y. Wei, Y. Ji, *Adv. Mater.* **2018**, *30*, 1801103.
- [225] M. K. McBride, A. M. Martinez, L. Cox, M. Alim, K. Childress, M. Beiswinger, M. Podgorski, B. T. Worrell, J. Killgore, C. N. Bowman, *Sci. Adv.* **2018**, *4*, eaat4634.
- [226] B. Ni, H.-L. Xie, J. Tang, H.-L. Zhang, E.-Q. Chen, *Chem. Commun.* **2016**, *52*, 10257.
- [227] Q. Yu, M. Li, J. Gao, P. Xu, Q. Chen, D. Xing, J. Yan, M. J. Zaworotko, J. Xu, Y. Chen, P. Cheng, Z. Zhang, *Angew. Chem., Int. Ed.* **2019**, *58*, 18634.
- [228] Q. Yu, X. Yang, Y. Chen, K. Yu, J. Gao, Z. Liu, P. Cheng, Z. Zhang, B. Aguila, S. Ma, *Angew. Chem.* **2018**, *130*, 10349.
- [229] F. Terao, M. Morimoto, M. Irie, *Angew. Chem., Int. Ed.* **2012**, *51*, 901.
- [230] H. Koshima, H. Nakaya, H. Uchimoto, N. Ojima, *Chem. Lett.* **2012**, *41*, 107.
- [231] Y. Huang, Q. Yu, C. Su, J. Jiang, N. Chen, H. Shao, *Actuators* **2021**, *10*, 298.
- [232] L. Qin, X. Liu, Y. Yu, *Adv. Opt. Mater.* **2021**, *9*, 2001743.
- [233] A. N. Koya, J. Cunha, K. A. Guerrero-Becerra, D. Garoli, T. Wang, S. Juodkazis, R. Proietti Zaccaria, *Adv. Funct. Mater.* **2021**, *31*, 2103706.
- [234] R. Fu, Y. Lu, W. Cheng, *Adv. Opt. Mater.* **2022**, *10*, 2101436.
- [235] Q. Guo, X. Zhang, *Compos. Part B Eng.* **2021**, *227*, 109434.
- [236] B.-B. Li, L. Ou, Y. Lei, Y.-C. Liu, *Nanophotonics* **2021**, *10*, 2799.
- [237] X. Sun, K. Y. Fong, C. Xiong, W. H. P. Pernice, H. X. Tang, *Opt. Express* **2011**, *19*, 22316.
- [238] K. Srinivasan, H. Miao, M. T. Rakher, M. Davanzo, V. Aksyuk, *Nano Lett.* **2011**, *11*, 791.
- [239] M. Li, W. H. P. Pernice, H. X. Tang, *Nat. Nanotechnol.* **2009**, *4*, 377.
- [240] J. Manley, D. J. Wilson, R. Stump, D. Grin, S. Singh, *Phys. Rev. Lett.* **2020**, *124*, 151301.
- [241] A. Tabatabaeian, S. Liu, P. Harrison, E. Schlangen, M. Fotouhi, *Compos. Part Appl. Sci. Manuf.* **2022**, *163*, 107236.
- [242] F. Pujol-Vila, R. Villa, M. Alvarez, *Front. Mech. Eng.* **2020**, *6*.
- [243] J. H.-C. Wang, B. P. Thampatty, *Biomech. Model. Mechanobiol.* **2006**, *5*, 1.
- [244] D. Sanahuja, P. Giménez-Gómez, N. Vigués, T. N. Ackermann, A. E. Guerrero-Navarro, F. Pujol-Vila, J. Sacristán, N. Santamaria, M. Sánchez-Contreras, M. Díaz-González, J. Mas, X. Muñoz-Berbel, *Lab Chip* **2015**, *15*, 1717.

- [245] E. Noviana, T. Ozer, C. S. Carrell, J. S. Link, C. McMahon, I. Jang, C. S. Henry, *Chem. Rev.* **2021**, 121, 11835.
- [246] J. Yang, S. Gurung, S. Bej, P. Ni, H. W. H. Lee, *Rep. Prog. Phys.* **2022**, 85, 036101.
- [247] P. Pitchappa, A. Kumar, S. Prakash, H. Jani, T. Venkatesan, R. Singh, *Adv. Mater.* **2019**, 31, 1808157.
- [248] S. G.-C. Carrillo, L. Trimby, Y.-Y. Au, V. K. Nagareddy, G. Rodriguez-Hernandez, P. Hosseini, C. Ríos, H. Bhaskaran, C. D. Wright, *Adv. Opt. Mater.* **2019**, 7, 1801782.
- [249] B. Gholipour, J. Zhang, K. F. MacDonald, D. W. Hewak, N. I. Zheludev, *Adv. Mater.* **2013**, 25, 3050.
- [250] B. Gholipour, D. Piccinotti, A. Karvounis, K. F. MacDonald, N. I. Zheludev, *Nano Lett.* **2019**, 19, 1643.
- [251] F. Ding, Y. Yang, S. I. Bozhevolnyi, *Adv. Opt. Mater.* **2019**, 7, 1801709.
- [252] M. Wuttig, H. Bhaskaran, T. Taubner, *Nat. Photonics* **2017**, 11, 465.
- [253] S. B. Campbell, Q. Wu, J. Yazbeck, C. Liu, S. Okhovatian, M. Radisic, *ACS Biomater. Sci. Eng.* **2021**, 7, 2880.
- [254] L. Davenport Huyer, A. D. Bannerman, Y. Wang, H. Savoji, E. J. Knee-Walden, A. Brissenden, B. Yee, M. Shoaib, E. Bobicki, B. G. Amsden, M. Radisic, *Adv. Healthcare Mater.* **2019**, 8, 1900245.
- [255] E. Sano, C. Mori, N. Matsuoka, Y. Ozaki, K. Yagi, A. Wada, K. Tashima, S. Yamasaki, K. Tanabe, K. Yano, Y.-S. Torisawa, *Micromachines* **2019**, 10, 793.
- [256] K. Domansky, J. D. Sliz, N. Wen, C. Hinojosa, G. Thompson, J. P. Fraser, T. Hamkins-Indik, G. A. Hamilton, D. Levner, D. E. Ingber, *Microfluid. Nanofluidics* **2017**, 21, 107.
- [257] D. Sticker, R. Geczy, U. O. Häfeli, J. P. Kutter, *ACS Appl. Mater. Interfaces* **2020**, 12, 10080.



Ferran Pujol-Vila earned his degree in Biology in 2010 from the Universitat Autònoma de Barcelona (UAB) (Spain). In 2017, he obtained his Ph.D. degree in Microbiology at Universitat Autònoma de Barcelona. In 2019, he joined the Institute of Microelectronics of Barcelona (IMB-CNM, CSIC) (Spain). Currently, he holds a Tecniospring Industry grant (co-financed by the H2020 Marie Skłodowska-Curie actions). After one year at the University of Antwerp (Belgium), he has recently joined the IMB-CNM. His research is focused on developing advanced Micro-Nanotechnologies for Life Science from fundamental research to clinical, industrial, and environmental applications.



Pau Güell-Grau obtained his degree in Nanoscience and Nanotechnology from Universitat Autònoma de Barcelona (Spain) in 2014. In 2021, he obtained the Ph.D. in materials science for his research on optical metamaterials for sensing and actuation devices. Since 2021, he works as a process integration engineer at the technology integration and prototyping department of IMEC.



ICREA Research Professor **José Nogués** earned his degree from the Universitat Autònoma de Barcelona (Spain) in 1986. After obtaining his Ph.D. at the KTH-Royal Institute of Technology in Stockholm (Sweden) in 1993, he moved to the University of California San Diego (USA) to complete his postdoctoral studies. He became an ICREA research professor in 2001. He is since 2006 group leader of the Magnetic Nanostructures group at the Catalan Institute of Nanoscience and Nanotechnology (ICN2) in Barcelona. His group seeks to improve the functional properties of diverse types of magnetic and magnetoplasmonic nanostructures for diverse applications.



Mar Alvarez is tenured researcher at the Institute of Microelectronics of Barcelona (IMB-CNM), where she works since 2015. She obtained her MSc and Ph.D. degrees in Physics from the Autònoma University of Madrid in 2000 and 2005, respectively. She carried out her Ph.D. at the Institute of Microelectronics of Madrid (IMM-CNM), working on nanomechanical biosensors. In 2006, she moved to Monash University, in Melbourne, for a two years postdoctoral stay. In 2008 she joined the Catalan Institute of Nanoscience and Nanotechnology (ICN2). She is focused in the development of optomechanical sensors and microfluidics devices for biomedical and environmental applications.



Borja Sepulveda received the Ph.D. degree in Physics from the Complutense University of Madrid in 2005. In 2006 he received the prestigious Vetenskapsrådet postdoctoral grant from the Swedish Research Council at Chalmers University (Sweden). In 2008 he joined the Institut Català de Nanociència i Nanotecnologia (ICN2). In 2012, he got a permanent CSIC research position at the ICN2 and in 2021 he moved to the Institute of Microelectronics of Barcelona (IMB-CNM-CSIC). His current research is focused on developing new active opto-magnetic nanostructures that can be remotely controlled and actuated with light and magnetic fields for biomedical and environmental applications.